

Journal of Biomedical Optics

BiomedicalOptics.SPIEDigitalLibrary.org

Optical and x-ray technology synergies enabling diagnostic and therapeutic applications in medicine

Brian W. Pogue
Brian C. Wilson

SPIE.

Brian W. Pogue, Brian C. Wilson, "Optical and x-ray technology synergies enabling diagnostic and therapeutic applications in medicine," *J. Biomed. Opt.* **23**(12), 121610 (2018), doi: 10.1117/1.JBO.23.12.121610.

Optical and x-ray technology synergies enabling diagnostic and therapeutic applications in medicine

Brian W. Pogue^{a,*} and Brian C. Wilson^b

^aDartmouth College, Thayer School of Engineering, Geisel School of Medicine, Hanover, New Hampshire, United States

^bUniversity of Toronto, Princess Margaret Cancer Centre/University Health Network, Toronto, Ontario, Canada

Abstract. X-ray and optical technologies are the two central pillars for human imaging and therapy. The strengths of x-rays are deep tissue penetration, effective cytotoxicity, and the ability to image with robust projection and computed-tomography methods. The major limitations of x-ray use are the lack of molecular specificity and the carcinogenic risk. In comparison, optical interactions with tissue are strongly scatter dominated, leading to limited tissue penetration, making imaging and therapy largely restricted to superficial or endoscopically directed tissues. However, optical photon energies are comparable with molecular energy levels, thereby providing the strength of intrinsic molecular specificity. Additionally, optical technologies are highly advanced and diversified, being ubiquitously used throughout medicine as the single largest technology sector. Both have dominant spatial localization value, achieved with optical surface scanning or x-ray internal visualization, where one often is used with the other. Therapeutic delivery can also be enhanced by their synergy, where radio-optical and optical-radio interactions can inform about dose or amplify the clinical therapeutic value. An emerging trend is the integration of nanoparticles to serve as molecular intermediates or energy transducers for imaging and therapy, requiring careful design for the interaction either by scintillation or Cherenkov light, and the nano-scale design is impacted by the choices of optical interaction mechanism. The enhancement of optical molecular sensing or sensitization of tissue using x-rays as the energy source is an important emerging field combining x-ray tissue penetration in radiation oncology with the molecular specificity and packaging of optical probes or molecular localization. The ways in which x-rays can enable optical procedures, or optics can enable x-ray procedures, provide a range of new opportunities in both diagnostic and therapeutic medicine. Taken together, these two technologies form the basis for the vast majority of diagnostics and therapeutics in use in clinical medicine. © 2018 Society of Photo-Optical Instrumentation Engineers (SPIE) [DOI: [10.1117/1.JBO.23.12.121610](https://doi.org/10.1117/1.JBO.23.12.121610)]

Keywords: x ray; optics; radiotherapy; imaging; spectroscopy; photo medicine.

Paper 180382SSVR received Jun. 25, 2018; accepted for publication Sep. 24, 2018; published online Oct. 22, 2018.

1 Introduction

Medical devices for diagnostics and therapeutics form the technological backbone of medicine, the most commonly utilized devices being radiological or optical in nature. Here we consider the evolving intersection between the two domains of radiodiagnostics/radiotherapeutics and photodiagnostics/phototherapeutics. It is of historical interest that, within a 10-year period, two of the earliest Nobel Prizes were awarded: to Roentgen for the discovery of x-rays in 1895 (Physics Prize) and to Finsen for the therapeutic applications of light in 1903 (Medicine & Physiology Prize). Of course, since that time, applications in therapy and diagnostics have flourished, with both domains having several more prize-winning advances and contributing in major ways to healthcare discoveries.

Considering first optical technologies, their greatest benefits revolve around the practical considerations of low cost, compactness, suitability for point-of-care use and positive safety profile, and especially for their fundamental properties of molecular sensitivity/specificity and wavelengths on the order of cellular/tissue structures. As a result, optical technologies are found throughout medical practice: in primary care, e.g., otoscopy, pulse oximetry, bilirubin monitoring in neonates; in diagnostics, e.g., endoscopic, dermatological, and ophthalmological imaging; in interventional guidance, e.g., in surgery

and cardiology; and in light-based therapeutics, e.g., surgical, dermatological and ophthalmological lasers, photodynamic therapy, and phototherapy. In addition, optical microscopy is the backbone of histopathology, whereas techniques such as flow cytometry and light-based biochemical analysis of tissues, cells, and body fluids are also essential parts of the diagnostic armamentarium.

Perhaps the most notable feature of optical biotechnologies is their technical diversity. This comes from a combination of many enabling optical components and materials (laser and non-laser light sources, fiber optics, photodetectors, and nonlinear optical materials) with the multiplicity of light-tissue interactions (absorption, elastic and inelastic scattering, polarizability, interference, etc.) that increasingly includes also the nonlinear domain using ultrafast laser pulses (ablation, multiphoton fluorescence, harmonic generation, stimulated Raman scattering, etc.). As a result, optical technologies tend to be highly specific to the organ, disease, and diagnosis, with different devices for different specialties. This contrasts with x-ray imaging and therapy systems that are much more general purpose, with a given device spanning a spectrum of clinical procedures. The clinical users of optical technologies also span a much wider range of specializations than do x-rays, which are primarily used within diagnostic radiology, radiation oncology, and cardiology. The scope of the two domains is expressed in terms of corresponding commercial markets [Fig. 1(a)]: perhaps surprisingly, optics-based tools have a much larger market footprint than do x-ray technologies. Additionally, the

*Address all correspondence to: Brian W. Pogue, E-mail: brian.w.pogue@dartmouth.edu

optical tools are expanding rapidly, due to interest in wearable and home-care technologies. The biomedical optics sector is expanding at double-digit annual rates.

The greatest challenge in photodiagnostics/therapeutics comes from the relatively poor tissue penetration of light (UV/visible/near-infrared), due to elastic scattering that is ~1000-fold higher than for x-rays [Fig. 1(b)]. Hence, optical techniques are restricted to directly accessible sites, such as the skin, eyes, and oral cavity, or require fiber-optic technologies in the form of endoscopic or intraoperative imaging, and for therapeutic light delivery to deep-seated tissues. Optical imaging through several cm of tissue thickness can be done at the cost of spatial resolution and is commonly used for interventional guidance, often in real time. The optical absorption and scattering properties of tissues are also variable over orders of magnitude from organ to organ and with disease, in a strongly wavelength-dependent manner, so that quantitative imaging and accurate energy targeting are extremely challenging, especially in 3-D. The absorption varies over six orders of magnitude in the visible range, but the effective attenuation is elastic-scatter dominated. Far-red and near-infrared (NIR) wavelengths have the highest tissue penetration, where hemoglobin, melanin, and water absorptions are low. Most optical imaging systems probe only a few mm below the illuminated tissue surface with high spatial resolution. Similarly, in phototherapeutics, high spatial localization can be achieved only near the exposed tissue surface or within a small distance from an interstitial light source, while up to about 1 cm of effective treatment range can typically be achieved using diffuse light.

By contrast, a major advantage of x-rays is their high tissue penetration [Fig. 1(b)]. Thus, x-ray imaging, either in the form of planar transmission techniques (static or dynamic/fluoroscopic) or computed tomography, can image all parts of the body with mm resolution. Likewise, MV x-rays from medical linear accelerators, guided by sophisticated pretreatment planning and enabled by dynamic collimation devices, allow precise therapeutic energy delivery to the target tissue (e.g., tumor). These capabilities are significantly enabled by the relatively small variations in the x-ray interaction coefficients within

and between tissues so that generic (water equivalent) values suffice for most treatment planning purposes and the radiation dose distribution can be uniform throughout the target volume. Importantly, however, x-rays lack molecular specificity as the interactions are at the atomic level. The carcinogenic risk in imaging and the off-target damage to normal tissues, are also significant limitations.

In general terms then, the question is: How can the complementary strengths of the radiation and optical domains be exploited to address the intrinsic and practical limitations of either domain? We will consider also how nanotechnologies, and specifically x-ray and/or photoactive nanoparticles, can facilitate this.

The use of optical technologies in radiation medicine has a long history, albeit in a limited sense. Examples include optical readout of x-ray film, scintillation materials for conversion of x-rays to light (and then to electrons) for signal detection in x-ray imaging systems, and dosimeters. More broadly, the potential uses can be considered separately for x-ray imaging and radiation therapy or can be broken down along the lines of physical, biochemical, or biological interactions.

Similarly, x-ray enabling of optical procedures has a broad range of applications, such as x-ray imaging to guide the placement or monitor the location of optical devices such as intravascular probes or capsule endoscopes. One of the most well-known examples is virtual colonoscopy by x-ray CT, where the surface topology of the colon is outlined by x-ray imaging to assess the need for real (i.e., optical) colonoscopy to remove or biopsy polyps. Intravascular placement of stents or other devices can also require hybrid x-ray and optical imaging tools.

The existing and potential interfaces between optical and radiation technologies and their applications may be split into (1) optical techniques used to enable diagnostic radiology and therapeutic radiation oncology and (2) x-ray technologies used to enable photodiagnostics and phototherapies, as shown in Fig. 2.

The idea depicted here is that there are two different ways to enhance clinical value by exploiting the complementary strengths of the optical and x-ray domains. Some aspects of

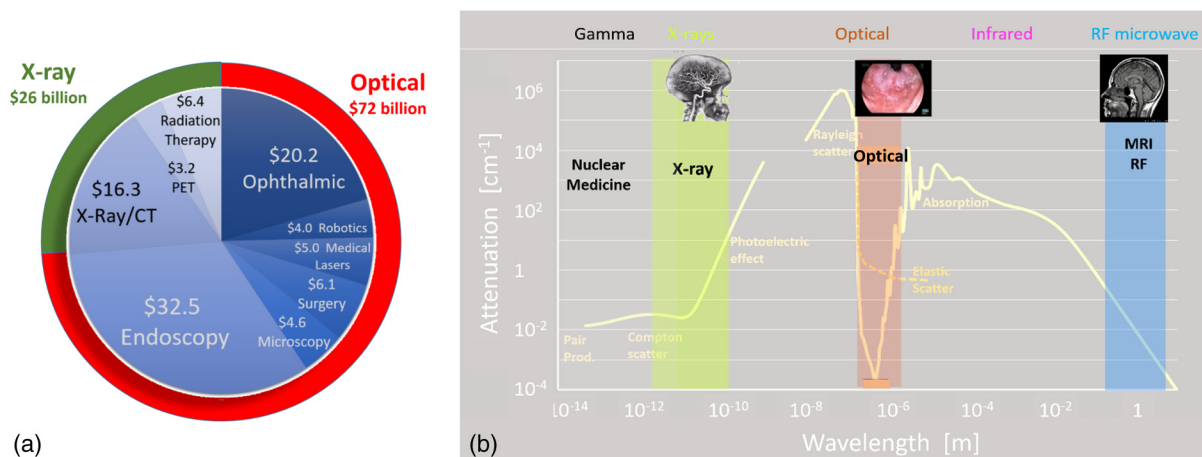


Fig. 1 (a) The global market sectors (US\$ billion/year) for optical and x-ray biomedical technologies.¹ (b) The attenuation mechanisms across the usable electromagnetic spectrum for water: note the steepness of absorption and scatter on either side of the red/near-infrared wavelength ranges, and the presence of high elastic scattering in this optical “window.” Medical imaging is done in each of the three areas of low attenuation, with x-ray, optical and magnetic resonance imaging techniques.

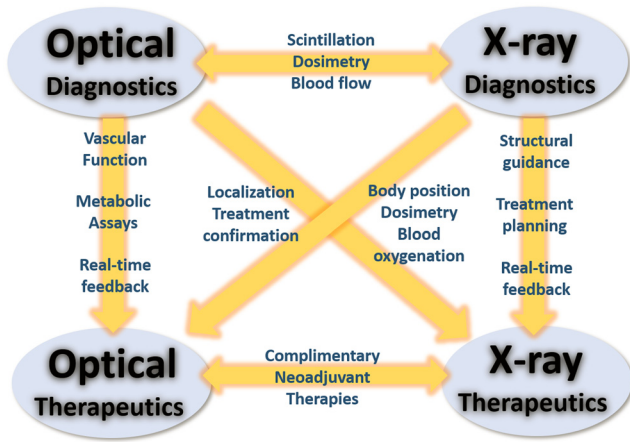


Fig. 2 Illustration of approaches to enhancing the cross-over between the x-ray and optical domains.

these interactions are well known and commonly used, such as cone beam x-ray CT localization of optical fibers delivering therapeutic light or optical (laser) alignment in radiotherapy delivery. However, many of the potential and under-developed synergies are at a more fundamental biochemical or nanotechnological level, as will be considered below. Figure 2 is intended to stimulate and guide thinking at a more abstract level about the spectrum of potential synergies along the diagnostics-to-therapeutic continuum (downward arrows) and the two-way reciprocity between optical and x-ray interactions (sideways arrows). Specific practical examples of the intersections are listed in Table 1.

2 Optics-Enabled X-Ray Techniques

In this section, we will consider the ways in which diagnostic and therapeutic applications of x-rays are, or could be, enabled or enhanced by optical technologies.

2.1 Current Medical X-Ray Technologies

Electronic x-ray production is among the most important discoveries in medicine. In imaging, the controlled production and detection of Kev x-rays provides optimal spatial resolution and contrast at minimum radiation dose.²⁻⁸ As shown in Fig. 3, x-ray imaging systems have a range of complexity that is related to the clinical applications, progressing from simple two-dimensional (2-D) projection imaging to 3-D volumetric or cross-sectional tomography to real-time fluoroscopic guidance of intervention procedures (e.g., vascular stent placement, aneurysm closure and tissue ablation, including by laser light). Optical detectors form the core of many x-ray sensor systems, although there have been major advances in the last decade toward detectors that use direct conversion of x-rays to electronically charge. Indirect detectors using intermediate optical processes continue to evolve from advances in materials science, including nanotechnology. The latter will be discussed further below.

In radiation therapy, MV x-ray beams and the resulting 3-D dose distributions are defined with mm accuracy throughout the target volume (e.g., tumor) and intervening tissues.⁹⁻¹⁹ Precision multileaf collimators control the lateral extent of the beam and allow shaped targeting. Combined with a rotating gantry and freedom of movement of the patient table, advanced inverse treatment planning algorithms allow the maximum uniform target dose with minimal dose to the intervening organs.

Table 1 Categories of interactions between optical and x-ray procedures, based along the lines of diagnostics and therapeutics (columns) and physical/technological, biological/functional, and biophysical/biochemical effects (rows).

		Optics enable x-rays		X-rays enable optics	
		Diagnostic radiology	Radiation oncology	Optical diagnostics	Optical therapeutics
Physical and technological	Physical	Alignment laser beams	Surface mapping	Measurement site localization/planning	Surgical localization and pretreatment planning
	Detector	Film, indirect imaging detectors, flat panel imagers	Detection/dosimetry film, portal imagers, point dosimeters	Real time guidance	Real time interventional guidance
	Interactive	Scintillation, indirect detectors	Gel dosimeters, water-tank imaging		
Biological and functional	Body position	Basic alignment	Surface mapping	Localization of internal anatomy	Assessing vascular occlusion
	Vascular	Vascular: Pulsatile flow, perfusion, parametric	Dosimetry verification QA of beam accuracy	Imaging in cardiovascular procedures	Assessing tissue necrosis
	Metabolic	Oxygenation, water, scatter changes, immune, RNA/DNA sensing	Blood oxygenation, molecular sensing		Complementary vascular and cellular treatments
Biophysical and biotech	Biophysical	Radio-luminescence	Cherenkov and scintillator-mediated molecular probes	X-ray activated optical reporters	Complementary cellular damage
	Nanotech	Molecular probes	Optical sensitization	X-ray-based molecular imaging	X-ray activated photosensitization

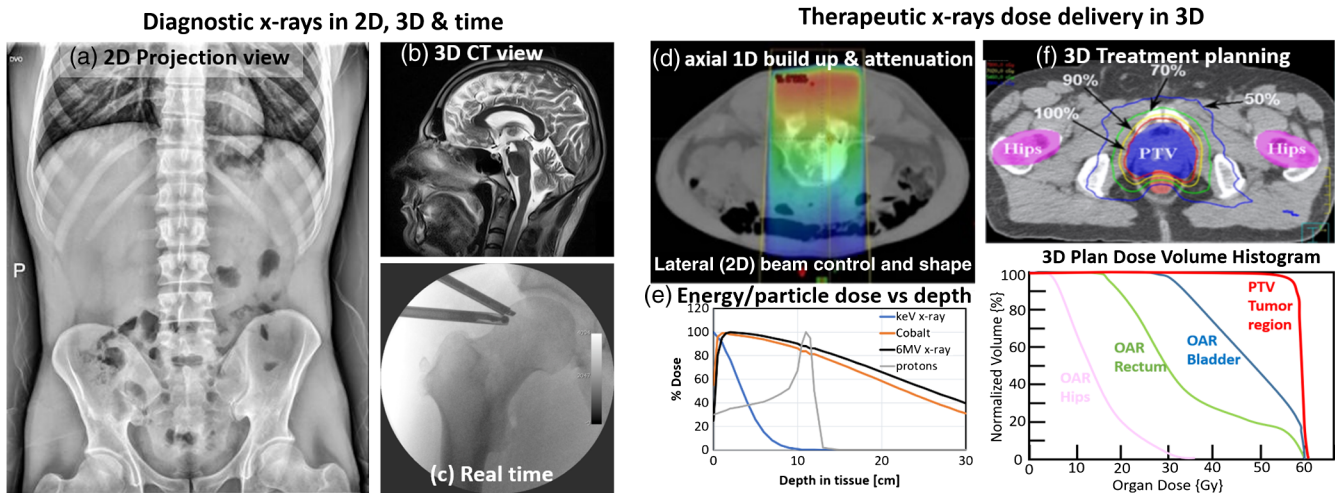


Fig. 3 X-ray diagnostic and therapy systems in 2-D and 3-D: diagnostic x-ray imaging systems are widely used in (a) 2-D and (b) 3-D imaging as well as (c) dynamic 2-D (“2.5-D”) during fluoroscopy-guided procedures. In radiotherapy, geometric precision of dose deposition is critical and (d) dose control is obtained laterally by beam collimators and (e) axially by the choice of the beam energy or particle type. Together these axial and lateral controls are used with computational treatment planning tools to optimize a dose plan (f) with a dose volume histogram that maximizes the % area of planning treatment volume while minimizing dose to organs at risk.

Optical tools have become pervasive throughout radiation oncology, with lasers used in almost every treatment unit for daily patient alignment^{20–22} and now surface mapping for patient setup and verification,²³ both shown in Fig. 4. Further information to aid in optimal treatment delivery comes from the original technology of (optical) film dosimetry as well as thermoluminescence.^{24–26} Optical gel dosimeters are under active development^{27–30} to enable accurate direct dose verification. Fiberoptic-based scintillation dosimetry has also been developed,^{31–34} with extension to scintillating fiber arrays for dose mapping,^{35,36} where the signal comes from the scintillator radioluminescence.

2.2 Emerging and Future Medical X-Ray Technologies Enabled by Optics

In x-ray diagnostics, the evolution of optical positioning devices will likely continue, with hybrid surface-mapping tools combined with time-gated imaging to reduce motion artifacts such as around the lungs or heart. These optical tools are now widespread throughout clinical medicine and likely to grow in more use. Optical measurements and imaging based on Cherenkov light from radionuclides have been reported in the last decade,^{38,39–43} with significant investigations into surface/subsurface imaging. The most promising applications to date have been in small-animal imaging, but initial clinical studies have also been reported,^{44,45} e.g., to detect tumor margins in surgical-specimens.^{46,47} Early-stage commercial prototypes have been developed. It is still not yet clear how this will impact clinical medicine, but trials are emerging now in margin detection and other surface detection needs in nuclear medicine.

In x-ray therapeutics, advances are being made using optics-based technologies and in exploiting intermediate photophysical or photochemical processes to enhance precision and efficacy. As shown in Fig. 4, these include fiber optic-based dosimetry

exploiting scintillation detection,³¹ online monitoring of tissue oxygenation status using hemoglobin spectroscopy⁴⁸ and, more recently, imaging the Cherenkov light generated in tissue by high-energy secondary electrons from MV x-ray beams during treatment. This last approach enables the irradiated tissue surface area to be directly visualized in real time and so is a promising addition to existing tools for quality control and precision x-ray dose delivery.^{49–51} While this is just in the early clinical trial stage, the potential for treatment monitoring seems promising, as discussed further below.

A complementary aspect of optics-enabled radiation therapy is radiosensitization. Efforts to exploit radiochemistry to increase the sensitivity of tumors relative to normal tissues have been ongoing for decades⁵² but have not translated into routine clinical practice. The greatest success has been in combining radiotherapy with chemotherapy, for example, using cisplatin and 5FU^{53,54} and other targeted adjuvant biological therapies to inhibit DNA repair⁵⁵ or to inhibit cell-signaling molecules.^{56,57} Physical radiosensitization using metal nanoparticles^{58,59} has shown some promise through the generation of additional secondary-electron dose. A recent development is the use of psoralens with x-ray activation as photochemical radiation sensitizers. Psoralens are used commonly for phototherapeutics in psoralen activation by ultraviolet A radiation (PUVA) treatment of benign skin diseases (e.g., psoriasis) where, upon activation by externally applied UVA light, they intercalate into DNA and prevent cell division. Mediated by the Cherenkov light generated by MV x-rays, psoralens have recently shown radiosensitizing properties for low-dose fractionated radiotherapy, both *in vitro* and in pre-clinical tumor models *in vivo*.^{60,61} This novel approach is thought to be based on fundamentally different mechanisms of action than conventional physical or chemical radiosensitizers. There are also potential synergistic interactions in x-ray-induced photosensitization using nanoparticles, as discussed below.

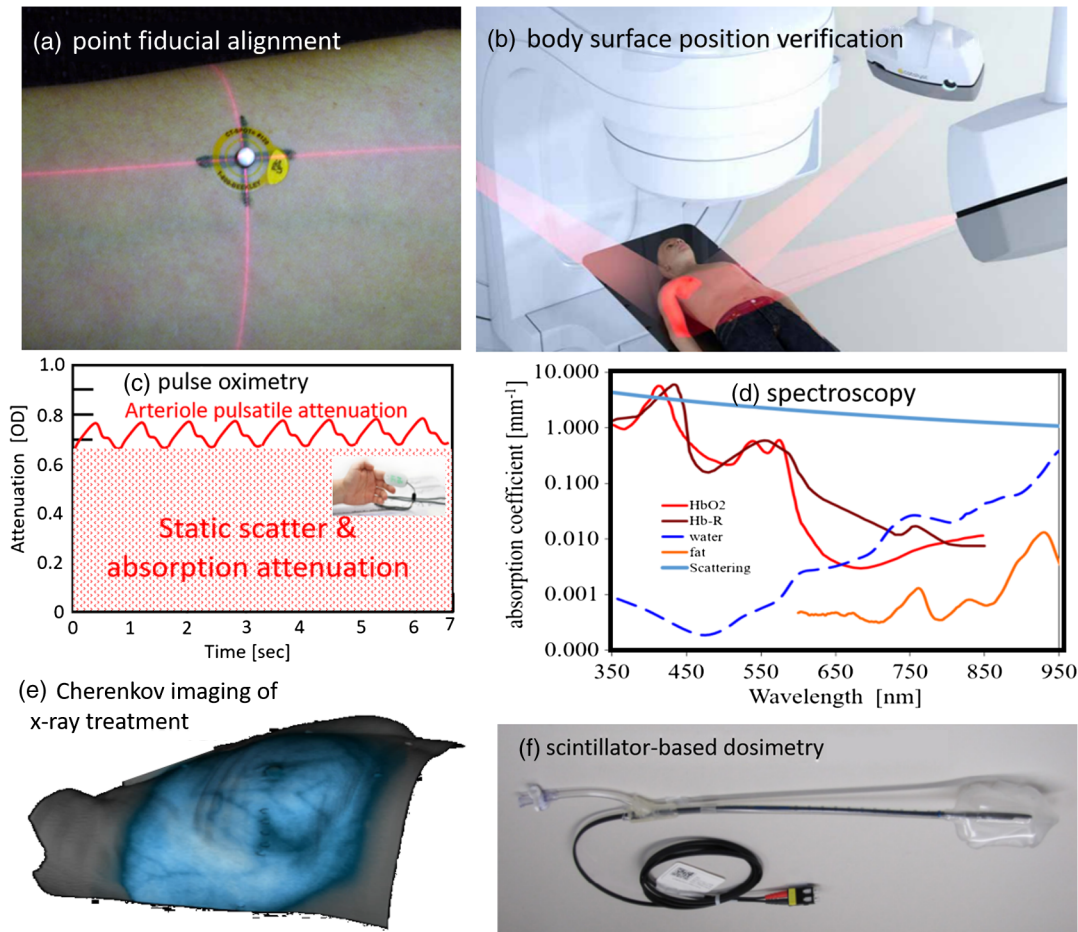


Fig. 4 Examples of optical technologies applied to radiation medicine. (a) Patient positioning by laser lines projected onto fiducial markers. (b) Surface projector/camera systems that use stereo vision or active illumination to map 3-D surfaces for patient position verification. (c) Measurement of blood oxygenation by pulse oximeter tracking the subtle attenuation changes from arteriole fluctuations. (d) Spectroscopic measurements from hemoglobin, water, fat or scattering to quantify constituents. (e) Direct Cherenkov imaging of radiation beams on tissue to verify delivery in real time. (f) Scintillation fiber-based dosimetry for accurate quantitative measurements of radiation *in situ* during radiotherapy.³⁷ © Institute of Physics and Engineering in Medicine. Reproduced by permission of IOP Publishing. All rights reserved.

3 X-Ray Enabled Optical Techniques

In this section, we will consider ways in which x-rays are or could be used to overcome existing limitations of photodiagnos- tics and phototherapeutics, particularly the low penetration of visible/NIR light in tissue.

3.1 Current Biomedical Optics Technologies

Photodiagnos- tics and phototherapeutics cover an extremely diverse set of technologies and clinical applications, so that this topic is not exhaustively covered here. Photodiagnostic techniques include: pulse oximetry based on optical spectroscopy of hemoglobin; ophthalmological, dermatological, and endoscopic imaging techniques *in vivo*; cytological and histopa- thological techniques *ex vivo* for disease detection, localization and staging; low-cost, point-of-care spectroscopic and imaging devices; systems for interventional guidance, particularly in surgery but also in applications such as wound care, as well as in radiotherapy as seen above. These optical technologies are often used stand-alone but increasingly are seen also in combination with other optical or nonoptical methods. Optical diagnostic

techniques/technologies can utilize many different light-tissue interactions, both linear (signal proportional to local light intensity) and emerging approaches that utilize nonlinear interactions. Either may be “label free,” i.e., based on endogenous biomolecular composition or tissue microstructure, or may use topically- or systemically administered exogenous molecular or nanoparticulate optical “reporters.” Opportunities and challenges in translating these various technologies into clinical use have been discussed in several recent papers.^{62–66}

The sensitivity and specificity of the optical signals from tis- sue are indicative of biochemical and/or ultrastructural features associated either with normal morphological/physiologic/ molecular processes or with changes in these diseases. The molecular sensitivity of optical diagnostics has been widely uti- lized with both endogenous and exogenous signals. Endogenous approaches include: volumetric diffuse reflectance or transmit- tance spectroscopy/spectral imaging based on a combination of absorption (biochemical content) and elastic scattering (tissue microstructure) and used for low-resolution tomography, vascu- lar perfusion, and blood-flow imaging; tissue autofluorescence from collagen, porphyrins and various metabolic cofactors;

Raman scattering that probes intra-molecular vibrational states; optical coherence tomography showing cross-sectional micro-heterogeneities in refractive index due to intercellular and intracellular membrane structures; and elastic-scattering spectroscopy in which the fine details of the diffuse optical spectrum depend on the nuclear size distribution that changes between normal and malignant cells (increased ploidy). Nonlinear optical imaging techniques, based on the interaction of ultrashort (fs) laser pulses with tissue, include multiphoton absorption and harmonic scattering that provides access to new cellular and extracellular features such as collagen ultrastructure and distribution in the extracellular matrix that is an important element in tumor growth and spread.^{67,68} Exogenous optical reporters may be disease-targeted, with correspondingly optimized instrumentation, to enable, e.g., mapping of blood perfusion/flow, metabolic enzyme activity, mineral content, pH, oxygen, or cell-signaling molecules.^{69–72} The advantage is that there is wide latitude in “designer” reporter molecules to probe specific biological functions. The use of nanoparticle-based optical reporters also increases the detection sensitivity and expands the range of biological targets.

An important recent trend has been the development of hardware and software for hybrid optical-radiation imaging tools, for example, x-ray CT combined with fluorescence or bioluminescence, where the former provides gross morphological information to help localize and quantify the optical signals.⁷³ To date, this has focused primarily on preclinical small-animal imaging,^{74,75–77} but some combinations could be moved into clinical applications, e.g., x-ray CT (or MRI, ultrasound)-guided fluorescence endoscopy or intravascular imaging. This could be achieved either by simply using the technologies independently or by true instrumental hybridization. Although not in the x-ray domain, an example of hybrid optical/nonoptical technologies is photoacoustic imaging where, after being spatially diffused by elastic scattering, short (ns) pulses of laser light are absorbed locally in the tissue by hemoglobin or exogenous agents, causing thermal expansion that in turn generates acoustic waves that are detected by ultrasound arrays.^{78–80} This is now moving rapidly into clinical translation, as it combines the depth capability of ultrasound with the molecular specificity of light.

Optical therapeutics similarly covers a very broad range of light-tissue interactions and corresponding technologies. The choice of wavelength and power density determines, which interaction mechanism is dominant (Fig. 5): biomodulation using red/NIR light at very low power densities ($\sim 0.01 \text{ Wcm}^{-2}$ continuous or long-pulse) that is likely mediated by triggering of endogenous metabolic pathways; photochemical treatments such as PUVA or photodynamic therapy that use photosensitizers and vis/NIR light ($\sim 0.1 \text{ Wcm}^{-2}$, continuous) to target mammalian cells (cancer/precancer, vascular diseases) or micro-organisms (localized infections); photothermal treatments ($\sim 1 \text{ Wcm}^{-2}$ continuous or $\sim \text{ms}$ pulsed) used in dermatology for the removal or suppression of blood vessels,⁸¹ hair, acne⁸² and tattoos⁸³ and for skin resurfacing,⁸⁴ and in other medical specialties for deeper treatments via endoscopic or interstitial fiber-optic light delivery for surgery and photocoagulation;^{85–88} photomechanical ablation of tissues, either via direct molecular bond breaking using UV lasers ($\sim 10^9$ to 10^{13} Wcm^{-2} , 10^{-13} to 10^{-9} s pulsed) for high-precision surgery such as corneal reshaping or by direct photophysical ejection of material ($\sim 10^5$ to 10^9 Wcm^{-2} , 10^{-8} to 10^{-5} s

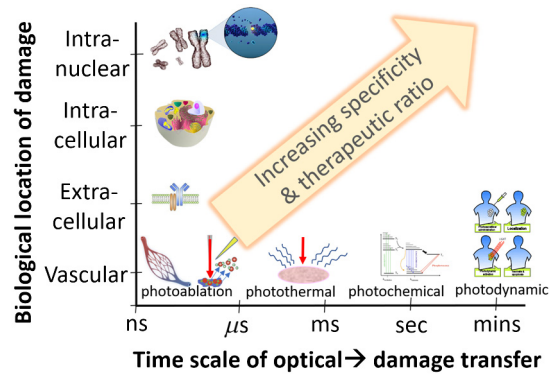


Fig. 5 Schematic of the dependence of the dominant photophysical interaction and resulting biological effects as a function of the light pulse length for a given optical energy density. Which effect is dominant also depends strongly on the localization of the optical absorber, and the specificity increases with more intraorganellar or nuclear targeting. Microlocalization and longer treatment times both generally provide superior specificity. Increasing specificity to tumor cells relative to the surrounding normal organs is key to maximizing the ‘therapeutic ratio’ of kill between tumor and normal tissue.

pulses) as used in laser surgery; photoelectromechanical ablation mediated by plasma and subsequent microbubble formation/collapse, as used, for example, to break kidney stones via fiber-optic light delivery ($\sim 10^3$ to 10^6 Wcm^{-2} , 0.001 to 1 s).^{85–88} Photochemical/photodynamic treatments using exogenous photoactive agents add a further degree of molecular specificity over and above the light targeting.^{89–91} These act through a variety of photobiological mechanisms: necrotic, apoptotic or autophagic tumor cell kill; damage to the microvasculature as in treatment of age-related macular degeneration,⁹² AMD;⁹³ and/or triggering of systemic immune responses.^{94,95} These cytotoxic effects are mediated by the photogeneration of excited radical states, such as singlet oxygen, which has also been a primary focus in the development of radiation-enabled phototherapeutics, as discussed below.

While ablative and thermal phototherapeutic technologies have had the greatest clinical and commercial penetration to date,⁹⁶ they tend to have limited tissue specificity, and the targeting is purely photophysical. This contrasts with photochemical/photodynamic treatments that have the potential for higher specificity based upon molecular or cellular uptake and retention of an activatable material. In general, treatments that shift from macroscopic to more microscopic or molecular biological targeting enhance the specificity of damage. For example, vascular damage is rather nonspecific, whereas cellular targeting can be more specific to the disease (e.g., cancer).⁹⁷ In particular, targeting of biomarkers, such as cell surface receptors in immunophotodynamic therapy,^{98,99–101} which are overexpressed in diseased cells, or localization of the photoactive material in intracellular organelles,¹⁰² including the nucleus,^{103,104} can enhance specificity of the therapy. Higher specificity leads to superior therapeutic ratio, because in the end cancer treatment is about the relative killing efficacy to the tumor relative to surrounding tissues or normal organs at risk of damage. This so-called therapeutic ratio determines the value of a treatment, in terms of tumor to normal tissue damage. Higher targeting specificity can improve this ratio significantly, and intelligent combinations of optical-x-ray therapies can maximize this.

3.2 Emerging and Future Biomedical Optical Technologies

3.2.1 Scintillation and Cherenkov light

The interaction of ionizing radiation with matter can take many forms, from radiochemistry to radioluminescence.^{105,106} Enhancement of radiation damage through molecular radiosensitizers and nanoparticles typically involves a complex cascade of many secondary events.¹⁰⁷ However, the events that directly precede molecular damage in therapy or molecular excitation in diagnostics can be preferentially enhanced by the addition of scintillation materials or by the intrinsic Cherenkov light generated in tissue.

Scintillation light is generated from direct transfer of energy from x-ray photons to electrons through the photoelectric effect in high atomic number materials. The resulting spectrum is common in the UV to blue-green wavelength range that has poor penetration in tissue, although red-emitting scintillation nanoparticles have been reported based on materials.^{108,109} Cherenkov light is produced by the interaction of charged particles traveling near the velocity of light in a dielectric material.¹¹⁰⁻¹¹² This emission is broadband, peaking in the UV-blue region and decaying as the inverse square of the wavelength. In water this is seen as blue light, but in tissue the blood absorption means that the red/NIR components propagate the furthest.

Both scintillation and Cherenkov light have been investigated for x-ray-mediated imaging and therapy as shown in Fig. 6 and appear promising as each x-ray photon can generate

$\sim 10^3$ Cherenkov photons or $\sim 10^3$ to 10^5 scintillation photons. For the latter, however, the volume fraction of the scintillator in tissue, as well as the spectral ranges, determine how much of the light is biologically effective. Most nanoscintillators could be administered in a pharmaceutical formulation, but at best would achieve $\sim 0.1\%$ volume fraction [Fig. 6(c)]. The quantum yield for nanoscintillation also decreases with x-ray photon energy so that there is a trade-off between light generation and x-ray penetration depth. By contrast, Cherenkov light is generated throughout the exposed tissue volume but has an energy threshold of ~ 220 KeV, with the output rising rapidly [Fig. 6(d)] and plateauing in the MeV range.

Many scintillators have been developed for KeV x-ray detection: in film screens, as indirect digital sensors and in CT. Inorganic CsI(Tl), CsF, BaF₂, CaWO₄ BGO, and LSO crystals have been used in a range of x-ray imaging applications.¹¹³⁻¹¹⁷ More recently, nanoparticles,¹¹⁸⁻¹²⁰ nanofibers,¹²¹ and nanowires¹²²⁻¹²⁴ have been investigated for imaging and sensing, exploiting their enhanced luminescence and short decay times that result in higher light output per unit radiation dose.

Historically, cancer patients have reported seeing (Cherenkov) light during therapeutic irradiation of the head with 6 to 18 MeV electrons,¹²⁵ and studies of therapeutic beams have shown that this light is readily detectable.^{49,126,127} Cherenkov emission from linacs, as well as from radioisotopes, has recently been investigated for *in vivo* optical molecular imaging using high-sensitivity camera systems.^{40,128,129-134} Gamma rays and MeV x-rays generate Cherenkov light via secondary electrons, and the intensity is governed only by the tissue refractive index and the secondary electron velocity.

3.2.2 Nanotechnology-mediated, x-ray-induced optical interactions

Advances in nanomaterials and their surface chemistry have diversified the options for generating light in tissue from x-rays. This includes direct x-ray interactions with metal or scintillating nanoparticles, as well as Cherenkov-mediated energy transfer from x-rays to UV/vis absorbers such as photocatalysts or photosensitizers as shown in Fig. 7.

In the therapeutic realm, there are reports of direct (i.e., non-light-mediated) activation of photodynamic sensitizers by x-rays, although the biological efficiency is modest.¹³⁵ Alternatively, scintillation nanoparticles have been investigated for light generation within target tissues upon x-ray irradiation to activate photosensitizers¹³⁹⁻¹⁴³ particularly for cancer treatment. Inorganic nanomaterials have been conjugated to organic photosensitizers in several studies to convert the x-ray photons to visible light that overlaps with the excitation spectrum of the photosensitizer.^{136,144-146} There may also direct resonant energy transfer between the excited scintillator and the photosensitizer molecules, which should have orders-of-magnitude higher efficiency than the two-step process of light generation followed by light absorption (see below).

Although not light-mediated and so outside the scope of this discussion, gold and platinum nanoparticles have been tested as radiation sensitizers,^{59,147} with dose-enhancement factors as high as about 50% in some reports.¹⁴⁸⁻¹⁵⁰ However, it is unclear if the enhancement is simply due to increased DNA damage¹⁵¹ as much of the sensitization is thought to be from short-range Auger electron emission that may not be collocated with the relevant biological targets. A major challenge in metal

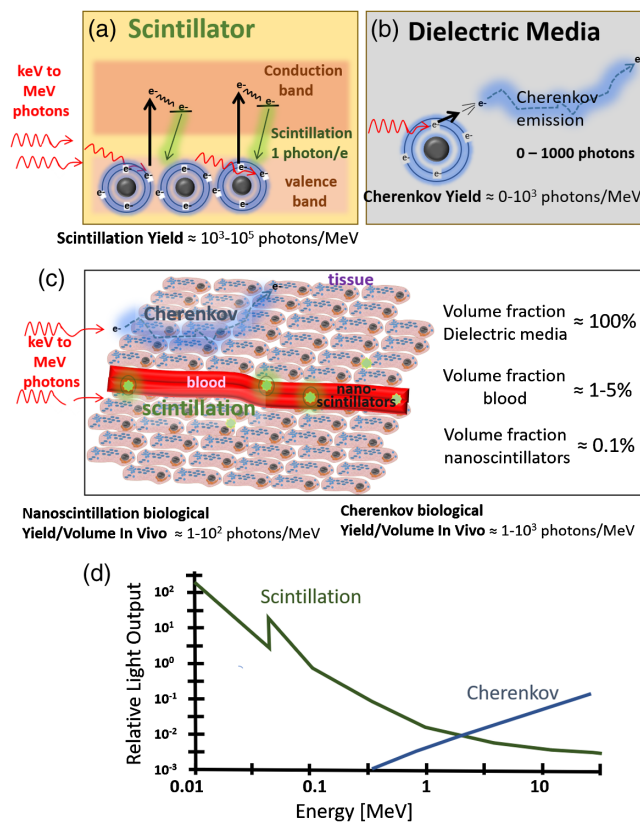


Fig. 6 Direct and secondary x-ray (or radionuclide) interactions producing light via (a) scintillation or (b) Cherenkov. (c) Order-of-magnitude estimates of the light yields in tissue. (d) Energy dependence of the two processes.

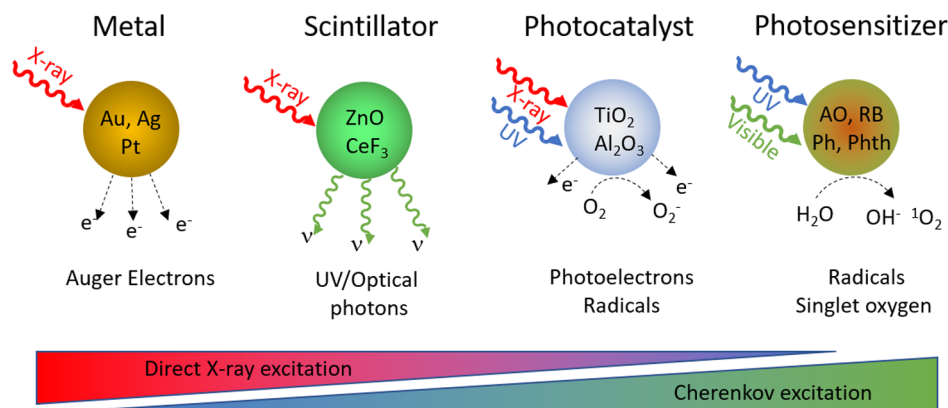


Fig. 7 X-ray interactions mediated by nanoparticles. (a) Metal nanoparticles generating direct electron emission, (b) nanoscintillators generating light that then activate photosensitizers, (c) photocatalyst mediating photoelectron and free-radical generation, and (d) direct generation of biologically active species from x-ray absorption in photosensitizers.^{58,135,136,137,138}

nanoparticle-based radiosensitization is to achieve robust enhancement at biologically relevant concentrations.

Photochemical therapies that utilize UV or short-wavelength visible light can also exploit x-ray Cherenkov.^{152,153} Likely candidate photosensitizers are UV-excited photocatalytic nanoparticles, such as TiO₂ or Al₂O₃. These have complex surface chemistry but can be designed to maximize electron-transfer that increases the efficacy.^{154,155} Alternatively, organic molecules such as porphyrins, bacteriochlorins, phthalocyanines, and smaller cyclic structures that absorb UV/violet-blue light operate through generation of biologically active free radicals or excited-state oxygen.¹⁵⁶⁻¹⁵⁸

Direct x-ray excitation is dominant in metals and scintillators, and there are multiple excitation mechanisms in photocatalysts and photosensitizer molecules. The choices to achieve maximum energy transfer here are not obvious because of the complexity of initiating events and the cascade of secondary events in the energy-transfer process.¹⁵⁹ Quantitative comparison of the physical efficiency and resulting biological effectiveness of these approaches remains challenging.

Higher biological efficacy is generally possible when the nanoparticles are modified to achieve better biotargeting or biodispersity to specific tissues, or to enhance catalysis or subsequent photosensitization as shown in Fig. 8. Selecting the optimal combination of specific excitation mechanisms with specific target localization is critical to advance these approaches.

3.2.3 Resonant energy transfer in x-ray-optical interactions

In the use of nanoparticles for which energy is transferred optically, the distance, *d*, between the scintillator and the acceptor photosensitizer molecule is critically important, as the probability of resonant energy transfer varies as 1/*R*⁶ [Fig. 9(a)]. This contrasts with the 1/*d*² dependence of nonresonant transfer or 1/*R* dependence of diffuse light [Fig. 9(c)]. Typical scintillators emit mainly in the UV/blue-green where the tissue attenuation is very high, so that strong colocalization of scintillator and photosensitizer minimizes this attenuation. Figures 9(d) and 9(e) show how the relative contributions of scintillation and Cherenkov light depend on the scintillator-photosensitizer separation.

The x-ray cross section of typical scintillators decreases with energy, so that Kev photons are more efficient than MeV photons. Conversely, the use of MV linacs is standard in radiotherapy as it provides superior tissue penetration, dose uniformity, skin sparing and beam control. The optimal trade-off between these factors has not been quantitatively determined and will markedly affect the clinical translatability of x-ray-mediated photosensitization, at least for treatment of deep-seated tumors.

For imaging applications where collecting molecular information is the objective, the various physical/biophysical factors involved are quantitatively somewhat different than in x-ray-mediated phototherapies, as optical signals can be detected

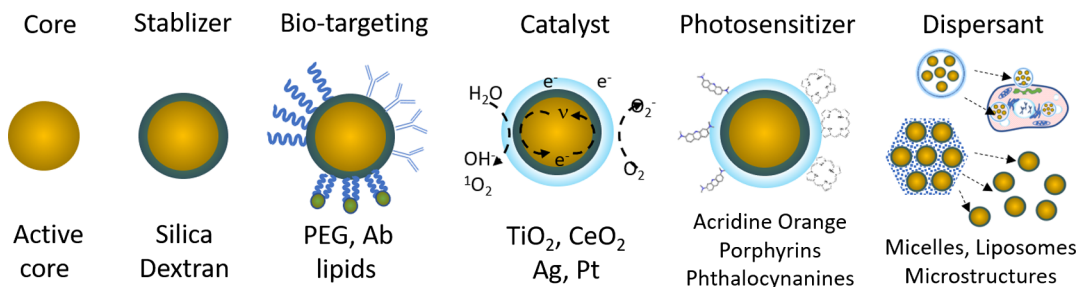


Fig. 8 Nanoparticle modifications, going from the active core, through stabilizing coatings, biomarker targeting, catalyst, or other active layers or coupling with light- or electronically-activated sensitizers, and incorporation into microstructures.

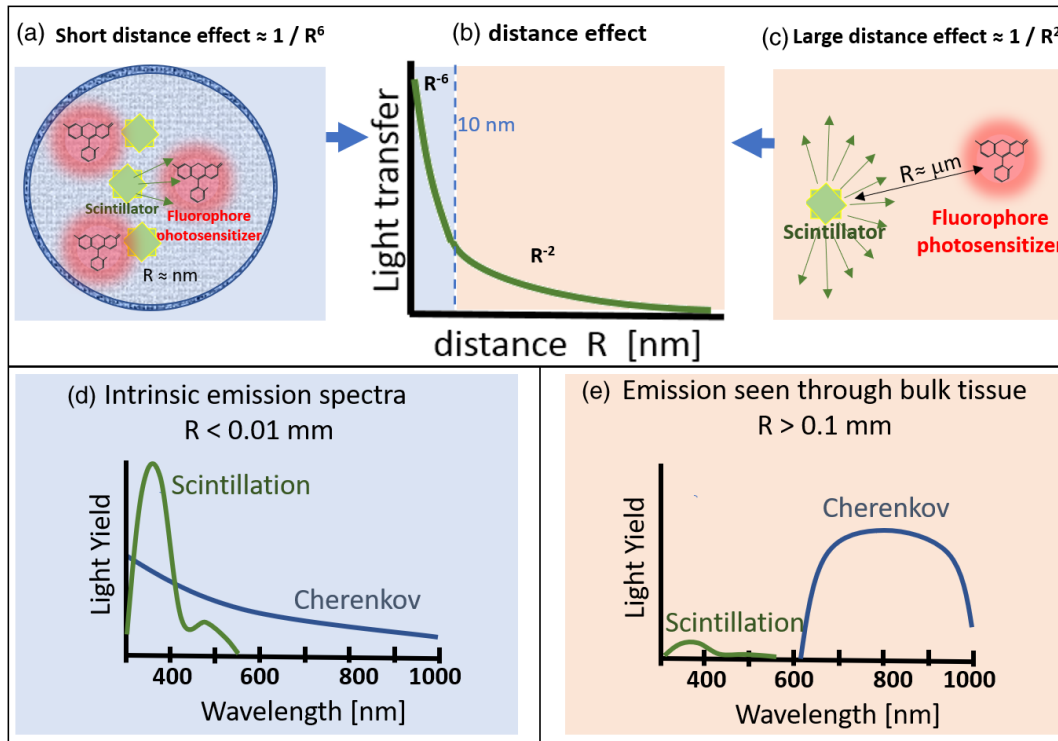


Fig. 9 Schematic of the dependence of effective photoactivation on the nanoscintillator-photosensitizer distance. (a) Resonant energy transfer at $\sim 10 \text{ nm}$, (c) nonresonant energy transfer through light emission by the donor and subsequent absorption by the acceptor, (b) combined distance dependence, with transition region near $R \sim 10 \text{ nm}$, (d) intrinsic scintillation and Cherenkov emission spectra in nearfield areas ($R \sim$ effective attenuation distance), and (e) preferential blue/green light attenuation in tissue.

down to the level of single photon counting. The largest fraction of radioisotope imaging is the use of PET scanning for disease staging, using ^{18}F -deoxyglucose, largely for metastasis staging. Hence, there is particular value in obtaining molecular information using external x-ray sources and longitudinal molecular imaging during a course of fractionated radiotherapy. However, an important wavelength factor must be considered in the use of external x-ray-generated Cherenkov light: the local light fluence from the emission is shown in Fig. 9(d), but the scattered fluence that will account for most of the signal generation is more like that shown in Fig. 9(e) so that the optimum molecular absorption spectrum is not well established.^{160,161}

Modulated MV beams and conformal radiotherapy techniques for Cherenkov excitation of molecular sensors are in place, so that clinical translation will depend on available low-toxicity luminescent agents that sense biologically-relevant factors, such as tissue oxygen or pH. The need to time-gate the light detection with linac activation currently limits the molecular lifetime to the microsecond range.¹⁶¹ However, methods to effectively sample fluorescent agents may be realized soon by deploying different classes or tumor-targeted microparticles or nanoparticles.

4 Molecular Therapy Applications Using X-Ray-Optical Interactions

Many types of doped fluoride nanoparticles have been combined with different photosensitizers (Fig. 10), with the most common objective of these x-ray-activated photodynamic therapy (XPDT) systems being to achieve tumor cell kill at low x-ray dose ($\sim < 10 \text{ Gy}$).^{142,162,163,164} One example is the

use of x-ray-generated Cherenkov light to excite psoralens [Fig. 10(a)] that were mentioned above in the context of optics-enabled radiation therapy for sensitization of fractionated radiotherapy. Psoralens have intrinsic nuclear uptake and, upon photoactivation, cross link to adenine and thymine residues in DNA, leading to proliferative cell death.¹⁶⁵ As recently suggested,¹⁶⁶ explicit nuclear targeting of photosensitizers combined with x-ray-generated Cherenkov or scintillation light may be particularly effective, as PDT mediated by direct light activation is known to have orders-of-magnitude greater cell kill for the same photosensitizer and light doses than when the photosensitizer is localized to extra-nuclear organelles.^{167,168} This may overcome the relatively low light levels of the scintillation and Cherenkov light.

Radio-sensitization has been investigated using the molecular dye acridine orange that intercalates into DNA upon interaction with x-rays to enhance cell damage.¹⁶⁹ An analogous but less potent effect is seen with the structurally similar methylene blue.¹⁷⁰ The use of acridine orange has advanced to initial clinical trials¹⁷¹⁻¹⁷⁴ and shows promise in sarcomas and other cancers. These effects likely come from Cherenkov light, although other damage effects may also be involved such as complementary biological insult unrelated to optical excitation of the molecule.

A second example [Fig. 10(b)] is the use of photosensitizers conjugated to CeF_3 scintillation nanocrystals, with MV linac irradiation. Both singlet oxygen generation and tumor cell kill *in vitro* have been demonstrated, and resonant energy transfer between the nanocrystals and the photosensitizer likely contributes to the efficacy. It is noteworthy that these studies utilized

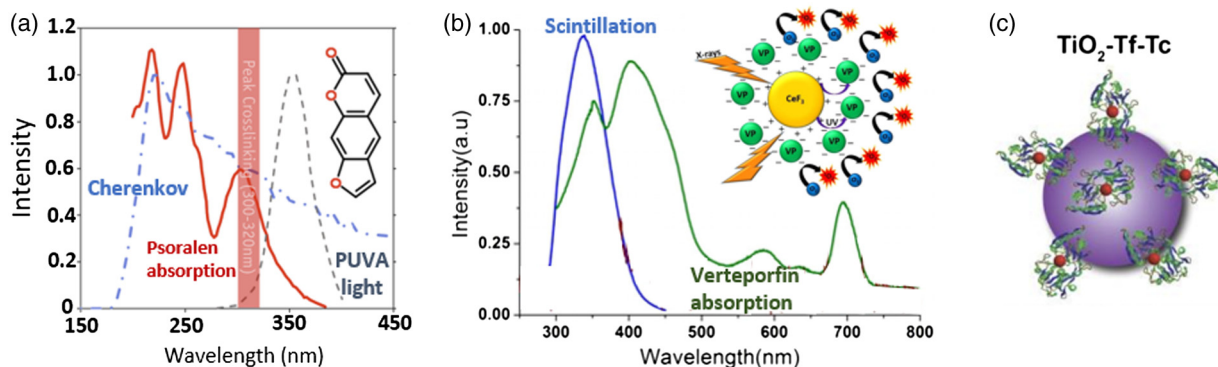


Fig. 10 Examples of x-ray-mediated phototherapeutics with psoralen photosensitization by Cherenkov light. (a) Spectral overlap of Cherenkov light and psoralen absorption, relative to the UVA light used in PUVA.⁶¹ (b) Scintillating CeF_3 nanocrystals coupled with photosensitizer (VP), with spectral overlap of the scintillation emission with the Soret band of VP, producing singlet-oxygen ($^1\text{O}_2$) from collisional quenching by molecular oxygen (O_2).¹³⁵ (c) X-ray Cherenkov excitation of TiO_2 nanoparticles from ^{64}Cu , producing cytotoxic photosensitization in tumor cells.¹³⁷

a clinically-approved photosensitizer [Verteporfin (VP)], which should facilitate future clinical translation. Several other preclinical nanoscintillator–photosensitizer studies have also shown efficacy *in vitro* and *in vivo* under MeV x-ray irradiation. Activation of photosensitizer from persistent luminescence nanoscintillators that emit light for several minutes after x-ray excitation has also been investigated.¹⁷⁵

Cherenkov-mediated PDT using high-energy (but low dose) x-ray beams has the significant advantage that accurate dose delivery allows greater precision and minimal “off-target” damage. An alternative approach is Cherenkov-mediated photosensitization using β -emitting radionuclides, as recently demonstrated^{137,176} in preclinical tumor models with surface-modified TiO_2 nanoparticles that act as UV-excited photocatalysts. The *in vivo* responses were also substantial, although both the TiO_2 and ^{65}Cu radionuclides were administered by direct intratumoral injection at high doses, which may restrict the clinical applicability.

5 Molecular Imaging from X-Ray–Optical Hybrid Systems

The use of x-rays to stimulate optical signals for diagnostic purposes has not been deployed clinically, yet there have been a series of promising developments in the past decade. The applications can be roughly divided according to whether the mechanism of light generation is scintillation or Cherenkov. The value of scintillation is that it can be quite bright and local, and the FRET or near-source effects shown in Fig. 7 can be utilized.

5.1 Scintillation-Based Molecular Imaging In Vivo

KeV x-rays used in radiography and computed tomography for anatomical imaging provide no molecular information. As indicated above, molecular imaging can be achieved based upon high-sensitivity CCD camera detection of the luminescence from scintillation materials activated by these x-rays within the tissue volume of interest.¹⁷⁷ X-ray-activated persistent luminescence imaging based on $\text{ZnGa}_2\text{O}_4:\text{Cr}$ nanoparticles has also been reported.¹⁷⁸ Full 3-D tomographic molecular imaging can be achieved by rotational excitation (Fig. 11), while x-ray luminescence computed tomography (XLCT)^{177,179,181} can simultaneously provide 3-D molecular and anatomical information.

To date, the luminescent agents have been largely inorganic and further development will be required to enable this approach to be used routinely. The narrow XLCT beams lead to a relatively long sampling time, so that a polycapillary lens has been utilized to generate a focused high-intensity micrometer-sized x-ray spot,^{182,183} enabling faster scanning without degrading spatial resolution or imaging depth. Cone-beam XLCT systems can also fully utilize the x-ray dose and shorten the scan time at the cost of reduced resolution.^{184–186} The benefit of XLCT is that the excitation signal is determined by the x-ray beam, so that high-resolution molecular (optical) imaging is possible even in the presence of significant light scattering. Further, this approach might be extended to single-point detectors by scanning the radiation beam, analogous to the geometry of a confocal scanning microscope. Advancing this method to clinical use would require low-toxicity, biologically relevant (microenvironment sensitive) contrast agents with good KeV x-ray cross-section.

5.2 Cherenkov-Based Molecular Imaging In Vivo

The discovery that higher KeV and MeV x-rays or gamma rays could excite molecular probes in tissue has illustrated how Cherenkov light could be used instead of scintillation or fluorescence.^{42,43,187–194} Scanned x-ray beam excitation of the Cherenkov light using the precision delivery of MeV radiation via multileaf collimators^{134,195} has been demonstrated (Fig. 12). Tomographic recovery is possible and the geometry between the x-ray beam and the detected luminescence remains to be fully optimized^{198,199} but could encompass raster scanning, line scanning or broad-beam excitation.^{134,195} A major benefit of using Cherenkov light is its broad emission spectrum, which allows a range of organic molecular dyes to be used as molecular probes. One example is based on a platinum-porphyrin dendrimer complex (PtG4) to image tissue pO_2 , while other luminescent agents absorbing in the visible range and detecting in the NIR range are also possible.¹⁶¹ The key to maximizing signal-to-noise in this approach has been the use of time-gated detection, where the noise and Cherenkov signal (in 4 μs bursts) from the original excitation beam can be eliminated. The current data suggest that it is feasible to sense nanomolar probe concentrations up to 30-mm deep in tissue.²⁰⁰ Additionally, there could be benefits from basic spectroscopic processing of the Cherenkov

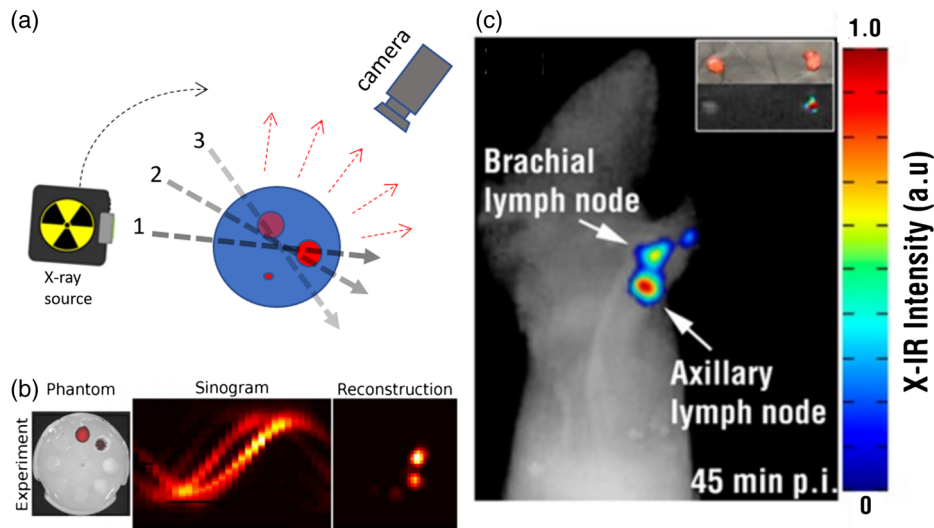


Fig. 11 X-ray luminescence computed tomography. (a) Rotational geometry of a KeV x-ray source. (b) resulting sinograms and reconstructed images of NIR emission in tissue phantoms.¹⁷⁹ (c) Example of *in vivo* planar imaging of lymph nodes using rare-earth-doped nanoscintillators at 45 min after injection.¹⁸⁰

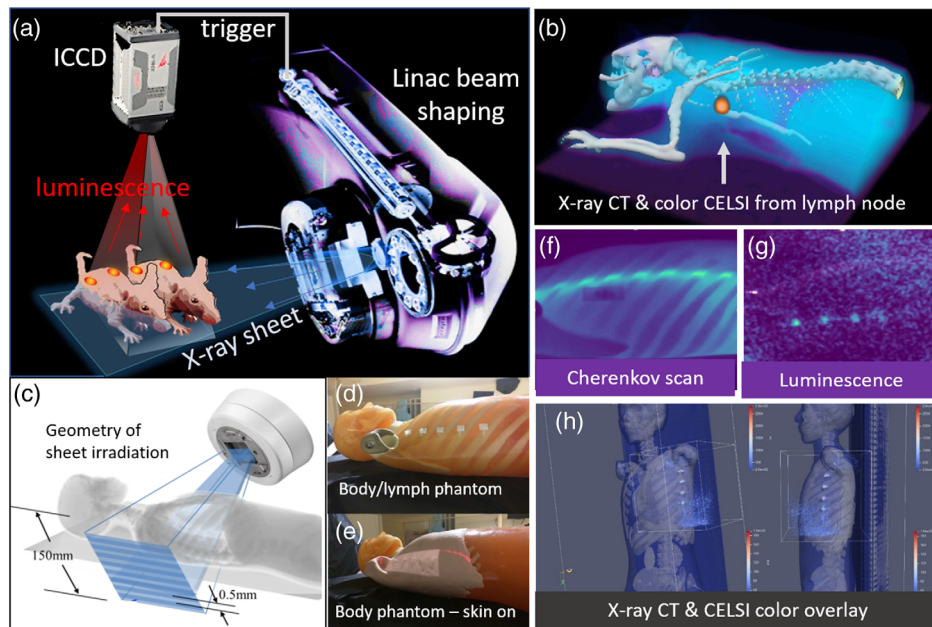


Fig. 12 Cherenkov luminescence molecular oxygen imaging. (a) Schematic of orthogonal line scanning from a 6 MV x-ray linac beam used to excite the luminescence that is captured by a time-synchronized camera. (b) Resulting reconstructed image *in vivo* from three orthogonal sheet scans.¹⁹⁶ (c) Human body phantom¹⁹⁷ with 1-D scanning, using (d) PtG4 samples on the chest cavity to simulate lymph nodes, and (e) covered with artificial skin. (f, g) Maximum-intensity projection Cherenkov and luminescence images. (h) CELSI image overlaid on the x-ray scans of the body phantom.

signal as shown recently.^{201,202} Sampling the tumor oxygen saturation in fractionated radiotherapy could be of value to adapt the treatment for more hypoxic tumors.

6 Discussion

These x-ray and optical intersections are multifaceted, with various established clinical and preclinical systems as well as many emerging applications. In this final section, we focus on separating them into x-rays enabling photomedicine and *vice versa*,

for both diagnostic and therapeutic values. The key values of the two lie in their mutual tissue penetration ability and the advanced nature of the commercialized technology in both areas.

6.1 X-Rays Enabling Optical Diagnostics

The range of existing applications using x-rays to enable optical diagnostics is relatively small, being largely in the positioning of endoscopic devices in which accurate targeting for biopsy is

particularly challenging. The most basic approach is an x-ray exam followed by an endoscopic or surgical exam. This is a seemingly trivial synergy, although widely practiced in clinical medicine today, as the x-ray provides the cross-sectional imaging by radiology, and the optical scan provides the surface imaging that is more directive of the tissue sampling such as biopsy or inspection.

A more ambitious approach is to use the x-rays as an energy source to excite a molecular reporter in a true hybrid diagnostic system, e.g., in scintillation- or radioluminescence-based imaging or Cherenkov-excited luminescence imaging (Figs. 11 and 12) using either kV or MV sources. This has been explored in only a few preclinical studies to date, but the use in biomedical research is likely to grow with advances in molecular sensors. As shown in Fig. 9, the packaging required to maximize the x-ray–optical effect is seemingly critical, with careful thought needed to maximize the likelihood of specific interaction between the emitted optical signal and any other reporter or detector. For example, scintillation-based probes are seemingly well suited to blue wavelengths and tight physical coupling to reporters, whereas Cherenkov-based probes are likely well excited throughout a volume, but only if red wavelengths are needed. Cherenkov probes coupled to isotope emitters have a lot of potential as self-emitting agents that can be used in molecular sensing or targeted therapy. As these are developed, further clinical implementations will require toxicity-tested and cost-effective molecular probes, for which the added information would significantly alter patient management.

6.2 Optics Enabling X-Ray Diagnostics

The range of applications where diagnostic optical approaches enable x-ray diagnostics is again relatively small at present, revolving mainly around positioning tools. Simple systems such as laser alignment and surface scanning are widely adopted in both diagnostic and therapeutic x-ray use for accurate patient positioning. Applications involving optical measurements of tissue oxygenation or blood/tissue metabolites are good examples where the molecular specificity of light would be complementary to the more structural information obtained from x-ray imaging. An example is Raman spectroscopy to characterize bone mineralization,^{203–206} providing complementary clinical information. Optical measurements that provide molecular information that might better inform the x-ray exam use or synchronization to biology, are also possible, providing added complementary information between optical diagnostics and x-ray diagnostics.

Further translation of clinical chemistry or immunochemistry principles to *in vivo* optical sensing may also occur and would be synergistic with 2-D or 3-D x-ray imaging in interventional applications that require information beyond the macroscopic morphological imaging that is provided by x-rays.

6.3 Optics Enabling X-Ray Therapeutics

There are many intersections where optical tools currently enable clinical x-ray therapy for positioning, dosimetry, and oximetry (Fig. 4) to improve the safety, efficacy, or management process. The delivery of clinical x-ray radiation therapy is actually completely dependent upon the accuracy that these positioning devices bring to the daily patient setup.

Procedures such as photodynamic therapy have niche roles in radiation medicine and there is evidence of complementary

efficacy between PDT and radiation treatments that have different subcellular targets and mechanisms of action²⁰⁷ or vasculature.⁹² This class of interactions can be thought of three ways: (1) complimentary adjuvant therapies, (2) synergistic therapies where one enhances the effect of the other, or (3) nanotechnology-mediated interaction where x-rays actually produce a photodynamic effect. The latter is a relatively new line of research (Figs. 11 and 12), achieving radiosensitization with the benefits of specificity and packaging of optical agents,^{157,158} and a number of efforts in materials chemistry have produced some extremely promising *in vivo* tumor killing results in the last few years. The key to advancing this approach to human use is to have nanoparticle agents that have low toxicity and are produced for human use, which is seemingly costly and currently uncertain. The same technologies for scintillator and Cherenkov imaging during radiotherapy at the macroscale will likely inform the development of microscale nanotherapeutic agents.

6.4 X-Rays Enabling Optical Therapeutics

The use of x-rays to enable optical interventions is commonplace, with open surgical, laparoscopic, orthopedical, gastroenterological, and cardiological procedures being guided by x-ray fluoroscopy or cone beam CT, exploiting the high penetration, bone contrast of x-rays, and soft tissue contrast of CT. Emerging applications where the x-rays are used as the energy source for phototherapies also take advantage of the deep penetration, through direct or indirect x-ray activation of optical agents such as molecular photodynamic agents or nanoparticles as described in Sec. 3.2. There are many nuances to optimize these techniques and to quantify the unique synergistic effects, particularly in the case of nanoparticles where many factors are involved: nanoparticle material and structure, x-ray cross-section, efficiency of energy transfer, subcellular localization and tissue level distribution (Figs. 7 and 8), and spectral overlap (Fig. 9).

7 Conclusions

The various examples discussed here of the ways in which optical and x-ray sciences and technologies intersect are intended both to illustrate the current state-of-the-art and, more importantly, to point to emerging trends. It should be clear that, while radiation medicine and photomedicine have evolved largely separately and have been driven by different technological capabilities and clinical/preclinical applications, there will be increasing synergistic overlap between these domains. Taken together, x-ray radiation technologies and optical technologies cover perhaps the vast majority of all advanced diagnostics and therapeutics in medicine today. Their intersections that fully utilize the strategic strengths of each will offer new opportunities in R&D, clinical translation and commercialization. These intersections also require thought about the training of new cadres of interdisciplinary thinkers and doers, such as those designing smart nanotechnologies for diagnostics or therapeutics, requiring expertise in surface and materials chemistry as well as aspects such as medicinal pharmacology and system engineering. These intersections should inspire new ventures and opportunities in a technology-driven approach to medicine.

Disclosures

Brian Pogue is the president and cofounder of DoseOptics LLC, a company developing radiation therapy dosimetry systems

capturing Cherenkov light imaging of dose delivery in radiation therapy.

Acknowledgments

This work has been funded by NIH grant R01 EB024498 and the Congressionally Directed Medical Research Program for Breast Cancer Research, under U.S. Army USAMRAA contract W81XWH-16-1-0004. Brian Pogue is grateful to members of the Optics in Medicine group at Dartmouth for numerous discussions that have helped shape this review paper. Brian Wilson also acknowledges the support of the Canadian Institutes of Health Research, the Cancer Research Society, and the Princess Margaret Cancer Foundation.

References

1. B. W. Pogue, "Optics of medical imaging," *SPIE Professional* (2018).
2. U. Baum et al., "Improvement of image quality of multislice spiral CT scans of the head and neck region using a raw data-based multidimensional adaptive filtering (MAF) technique," *Eur. Radiol.* **14**(10), 1873–1881 (2004).
3. T. Fuchs, M. Kachelriess, and W. A. Kalender, "Direct comparison of a xenon and a solid-state CT detector system: measurements under working conditions," *IEEE Trans. Med. Imaging* **19**(9), 941–948 (2000).
4. M. Kachelriess and W. A. Kalender, "Presampling, algorithm factors, and noise: considerations for CT in particular and for medical imaging in general," *Med. Phys.* **32**(5), 1321–1334 (2005).
5. W. A. Kalender, A. Polacin, and C. Suss, "A comparison of conventional and spiral CT: an experimental study on the detection of spherical lesions," *J. Comput. Assist. Tomogr.* **18**(2), 167–176 (1994).
6. Y. Kyriakou et al., "Impact of the z-flying focal spot on resolution and artifact behavior for a 64-slice spiral CT scanner," *Eur. Radiol.* **16**(6), 1206–1215 (2006).
7. M. J. Paulus et al., "A review of high-resolution x-ray computed tomography and other imaging modalities for small animal research," *Lab Anim. (NY)* **30**(3), 36–45 (2001).
8. G. Pang and J. A. Rowlands, "Development of high quantum efficiency flat panel detectors for portal imaging: intrinsic spatial resolution," *Med. Phys.* **29**(10), 2274–2285 (2002).
9. T. LoSasso et al., "The use of a multi-leaf collimator for conformal radiotherapy of carcinomas of the prostate and nasopharynx," *Int. J. Radiat. Oncol. Biol. Phys.* **25**(2), 161–170 (1993).
10. J. R. Kerns, N. Childress, and S. F. Kry, "A multi-institution evaluation of MLC log files and performance in IMRT delivery," *Radiat. Oncol.* **9**, 176 (2014).
11. J. I. Kim et al., "The sensitivity of gamma-index method to the positioning errors of high-definition MLC in patient-specific VMAT QA for SBRT," *Radiat. Oncol.* **9**, 167 (2014).
12. D. W. Litzenberg, J. M. Moran, and B. A. Fraass, "Incorporation of realistic delivery limitations into dynamic MLC treatment delivery," *Med. Phys.* **29**(5), 810–820 (2002).
13. Y. Liu et al., "Delivery of four-dimensional radiotherapy with TrackBeam for moving target using an AccuKnife dual-layer MLC: dynamic phantoms study," *J. Appl. Clin. Med. Phys.* **10**(2), 2926 (2009).
14. K. Otto and B. G. Clark, "Enhancement of IMRT delivery through MLC rotation," *Phys. Med. Biol.* **47**(22), 3997–4017 (2002).
15. J. M. Park et al., "The effect of MLC speed and acceleration on the plan delivery accuracy of VMAT," *Br. J. Radiol.* **88**(1049), 20140698 (2015).
16. R. A. Popple and I. A. Brezovich, "Dynamic MLC leaf sequencing for integrated linear accelerator control systems," *Med. Phys.* **38**(11), 6039–6045 (2011).
17. P. Rowshanfarzad et al., "A comprehensive study of the mechanical performance of gantry, EPID and the MLC assembly in Elekta linacs during gantry rotation," *Br. J. Radiol.* **88**(1051), 20140581 (2015).
18. C. B. Saw et al., "Commissioning and quality assurance for MLC-based IMRT," *Med. Dosim.* **26**(2), 125–133 (2001).
19. M. Woo et al., "Commissioning, evaluation, quality assurance and clinical application of a virtual micro MLC technique," *Med. Phys.* **30**(2), 138–143 (2003).
20. C. Westbrook, J. Gildersleve, and J. Yarnold, "Quality assurance in daily treatment procedure: patient movement during tangential fields treatment," *Radiother. Oncol.* **22**(4), 299–303 (1991).
21. N. J. Yue et al., "Patterns of intrafractional motion and uncertainties of treatment setup reference systems in accelerated partial breast irradiation for right- and left-sided breast cancer," *Pract. Radiat. Oncol.* **4**(1), 6–12 (2014).
22. N. J. Yue et al., "Intrafractional target motions and uncertainties of treatment setup reference systems in accelerated partial breast irradiation," *Int. J. Radiat. Oncol. Biol. Phys.* **79**(5), 1549–1556 (2011).
23. A. P. Shah et al., "Clinical evaluation of interfractional variations for whole breast radiotherapy using 3-dimensional surface imaging," *Pract. Radiat. Oncol.* **3**(1), 16–25 (2013).
24. M. Bardies and P. Pihet, "Dosimetry and microdosimetry of targeted radiotherapy," *Curr. Pharm. Des.* **6**(14), 1469–1502 (2000).
25. N. D. MacDougall, W. G. Pitchford, and M. A. Smith, "A systematic review of the precision and accuracy of dose measurements in photon radiotherapy using polymer and Fricke MRI gel dosimetry," *Phys. Med. Biol.* **47**(20), R107–R121 (2002).
26. B. Mijnheer et al., "In vivo dosimetry in external beam radiotherapy," *Med. Phys.* **40**(7), 070903 (2013).
27. S. Bosi et al., "Initial investigation of a novel light-scattering gel phantom for evaluation of optical CT scanners for radiotherapy gel dosimetry," *Phys. Med. Biol.* **52**(10), 2893–2903 (2007).
28. T. Olding, O. Holmes, and L. J. Schreiner, "Cone beam optical computed tomography for gel dosimetry I: scanner characterization," *Phys. Med. Biol.* **55**(10), 2819–2840 (2010).
29. T. Olding et al., "Small field dose delivery evaluations using cone beam optical computed tomography-based polymer gel dosimetry," *J. Med. Phys.* **36**(1), 3–14 (2011).
30. T. Olding and L. J. Schreiner, "Cone-beam optical computed tomography for gel dosimetry II: imaging protocols," *Phys. Med. Biol.* **56**(5), 1259–1279 (2011).
31. A. S. Beddar, N. Suchowerska, and S. H. Law, "Plastic scintillation dosimetry for radiation therapy: minimizing capture of Cerenkov radiation noise," *Phys. Med. Biol.* **49**(5), 783–790 (2004).
32. L. Archambault et al., "Plastic scintillation dosimetry: optimal selection of scintillating fibers and scintillators," *Med. Phys.* **32**(7), 2271–2278 (2005).
33. L. Archambault et al., "Toward a real-time in vivo dosimetry system using plastic scintillation detectors," *Int. J. Radiat. Oncol. Biol. Phys.* **78**(1), 280–287 (2010).
34. P. Z. Liu et al., "Plastic scintillation dosimetry: comparison of three solutions for the Cerenkov challenge," *Phys. Med. Biol.* **56**(18), 5805–5821 (2011).
35. V. Collomb-Patton et al., "The DOSIMAP, a high spatial resolution tissue equivalent 2D dosimeter for LINAC QA and IMRT verification," *Med. Phys.* **36**(2), 317–328 (2009).
36. A. M. Frelin et al., "The DosiMap, a new 2D scintillating dosimeter for IMRT quality assurance: characterization of two Cerenkov discrimination methods," *Med. Phys.* **35**(5), 1651–1662 (2008).
37. L. Beaulieu and S. Beddar, "Review of plastic and liquid scintillation dosimetry for photon, electron and proton therapy," *Phys. Med. Biol.* **61**, R305–R343 (2016).
38. C. Li, G. S. Mitchell, and S. R. Cherry, "Cerenkov luminescence tomography for small-animal imaging," *Opt. Lett.* **35**(7), 1109–1111 (2010).
39. R. Robertson et al., "Optical imaging of Cerenkov light generation from positron-emitting radiotracers," *Phys. Med. Biol.* **54**(16), N355–N365 (2009).
40. A. Ruggiero et al., "Cerenkov luminescence imaging of medical isotopes," *J. Nucl. Med.* **51**(7), 1123–1130 (2010).
41. A. E. Spinelli et al., "Cerenkov radiation allows in vivo optical imaging of positron emitting radiotracers," *Phys. Med. Biol.* **55**(2), 483–495 (2010).
42. D. Thorek et al., "Cerenkov imaging—a new modality for molecular imaging," *Am. J. Nucl. Med. Mol. Imaging* **2**(2), 163–173 (2012).
43. S. Das, D. L. Thorek, and J. Grimm, "Cerenkov imaging," *Adv. Cancer Res.* **124**, 213–234 (2014).
44. A. E. Spinelli and F. Boschi, "Human Cerenkov imaging using 18F-FDG," *J. Nucl. Med.* **55**(3), 523–523 (2014).

45. T. M. Shaffer, C. M. Drain, and J. Grimm, "Optical imaging of ionizing radiation from clinical sources," *J. Nucl. Med.* **57**(11), 1661–1666 (2016).
46. M. R. Grootendorst et al., "Cherenkov luminescence imaging (CLI) for image-guided cancer surgery," *Clin. Transl. Imaging* **4**(5), 353–366 (2016).
47. M. R. Grootendorst et al., "Intraoperative assessment of tumor resection margins in breast-conserving surgery using (18)F-FDG Cherenkov luminescence imaging: a first-in-human feasibility study," *J. Nucl. Med.* **58**(6), 891–898 (2017).
48. F. Hu et al., "Oxygen and Perfusion kinetics in response to fractionated radiation therapy in fadu head and neck cancer xenografts are related to treatment outcome," *Int. J. Radiat. Oncol. Biol. Phys.* **96**(2), 462–469 (2016).
49. A. K. Glaser et al., "Optical dosimetry of radiotherapy beams using Cherenkov radiation: the relationship between light emission and dose," *Phys. Med. Biol.* **59**(14), 3789–3811 (2014).
50. A. K. Glaser et al., "Optical cone beam tomography of Cherenkov-mediated signals for fast 3D dosimetry of x-ray photon beams in water," *Med. Phys.* **42**(7), 4127–4136 (2015).
51. R. Zhang et al., "Beam and tissue factors affecting Cherenkov image intensity for quantitative entrance and exit dosimetry on human tissue," *J. Biophotonics* **10**(5), 645–656 (2017).
52. T. Paunesku et al., "Radiosensitization and nanoparticles," *Cancer Treat. Res.* **166**, 151–171 (2015).
53. N. Ohri, A. P. Dicker, and Y. R. Lawrence, "Can drugs enhance hypofractionated radiotherapy? A novel method of modeling radiosensitization using in vitro data," *Int. J. Radiat. Oncol. Biol. Phys.* **83**(1), 385–393 (2012).
54. F. L. Reboul, "Radiotherapy and chemotherapy in locally advanced non-small cell lung cancer: preclinical and early clinical data," *Hematol. Oncol. Clin. N. Am.* **18**(1), 41–53 (2004).
55. S. H. Yang et al., "Perspectives on the combination of radiotherapy and targeted therapy with DNA repair inhibitors in the treatment of pancreatic cancer," *World J. Gastroenterol.* **22**(32), 7275–7288 (2016).
56. M. Baumann et al., "EGFR-targeted anti-cancer drugs in radiotherapy: preclinical evaluation of mechanisms," *Radiother. Oncol.* **83**(3), 238–248 (2007).
57. E. T. Shinohara and A. Maity, "Increasing sensitivity to radiotherapy and chemotherapy by using novel biological agents that alter the tumor microenvironment," *Curr. Mol. Med.* **9**(9), 1034–1045 (2009).
58. S. Her, D. A. Jaffray, and C. Allen, "Gold nanoparticles for applications in cancer radiotherapy: mechanisms and recent advancements," *Adv. Drug Delivery Rev.* **109**, 84–101 (2017).
59. K. Kobayashi et al., "Enhancement of radiation effect by heavy elements," *Mutat. Res.* **704**(1–3), 123–131 (2010).
60. M. Oldham et al., "X-ray psoralen activated cancer therapy (X-PACT)," *PLoS One* **11**(9), e0162078 (2016).
61. S. W. Yoon et al., "Enhancing radiation therapy through cherenkov light-activated phototherapy," *Int. J. Radiat. Oncol. Biol. Phys.* **100**(3), 794–801 (2018).
62. P. Crow et al., "Optical diagnostics in urology: current applications and future prospects," *BJU Int.* **92**(4), 400–407 (2003).
63. S. X. Han et al., "Molecular beacons: a novel optical diagnostic tool," *Arch. Immunol. Ther. Exp.* **61**(2), 139–148 (2013).
64. H. C. Lowe et al., "Intracoronary optical diagnostics current status, limitations, and potential," *JACC Cardiovasc. Interv.* **4**(12), 1257–1270 (2011).
65. A. Sahu and C. M. Krishna, "Optical diagnostics in oral cancer: an update on Raman spectroscopic applications," *J. Cancer Res. Ther.* **13**(6), 908–915 (2017).
66. T. Upile et al., "Head and neck optical diagnostics: vision of the future of surgery," *Head Neck Oncol.* **1**, 25 (2009).
67. R. Tanaka et al., "In vivo visualization of dermal collagen fiber in skin burn by collagen-sensitive second-harmonic-generation microscopy," *J. Biomed. Opt.* **18**(6), 061231 (2013).
68. P. P. Provenzano et al., "Collagen reorganization at the tumor-stromal interface facilitates local invasion," *BMC Med.* **4**(1), 38 (2006).
69. R. Alford et al., "Molecular probes for the in vivo imaging of cancer," *Mol. Biosyst.* **5**(11), 1279–1291 (2009).
70. D. R. Elias et al., "In vivo imaging of cancer biomarkers using activatable molecular probes," *Cancer Biomark* **4**(6), 287–305 (2008).
71. M. Y. Berezin et al., "Rational approach to select small peptide molecular probes labeled with fluorescent cyanine dyes for in vivo optical imaging," *Biochemistry* **50**(13), 2691–2700 (2011).
72. P. Sarder, D. Maji, and S. Achilefu, "Molecular probes for fluorescence lifetime imaging," *Bioconjug. Chem.* **26**(6), 963–974 (2015).
73. D. M. McClatchy, 3rd et al., "Molecular dyes used for surgical specimen margin orientation allow for intraoperative optical assessment during breast conserving surgery," *J. Biomed. Opt.* **20**(4), 040504 (2015).
74. D. Hyde et al., "Performance dependence of hybrid x-ray computed tomography/fluorescence molecular tomography on the optical forward problem," *J. Opt. Soc. Am. A* **26**(4), 919–923 (2009).
75. A. Ale et al., "FMT-XCT: in vivo animal studies with hybrid fluorescence molecular tomography-x-ray computed tomography," *Nat. Methods* **9**(6), 615–620 (2012).
76. P. Mohajerani et al., "FMT-PCCT: hybrid fluorescence molecular tomography-x-ray phase-contrast CT imaging of mouse models," *IEEE Trans. Med. Imaging* **33**(7), 1434–1446 (2014).
77. D. Kepshire et al., "A microcomputed tomography guided fluorescence tomography system for small animal molecular imaging," *Rev. Sci. Instrum.* **80**(4), 043701 (2009).
78. R. O. Esenaliev, "Optoacoustic diagnostic modality: from idea to clinical studies with highly compact laser diode-based systems," *J. Biomed. Opt.* **22**(9), 091512 (2017).
79. D. Grosenick et al., "Review of optical breast imaging and spectroscopy," *J. Biomed. Opt.* **21**(9), 091311 (2016).
80. J. A. Guggenheim et al., "Photoacoustic imaging of human lymph nodes with endogenous lipid and hemoglobin contrast," *J. Biomed. Opt.* **20**(5), 050504 (2015).
81. J. K. Chen et al., "An overview of clinical and experimental treatment modalities for port wine stains," *J. Am. Acad. Dermatol.* **67**(2), 289–304 (2012).
82. H. S. Lee et al., "Fractional photothermolysis for the treatment of acne scars: a report of 27 Korean patients," *J. Dermatol. Treat.* **19**(1), 45–49 (2008).
83. G. Pfirrmann et al., "Tattoo removal—state of the art," *J. Ger. Soc. Dermatol.* **5**(10), 889–897 (2007).
84. D. L. Johnson and F. Paletta, "Skin resurfacing procedures of the upper face," *Atlas Oral Maxillofac. Surg. Clin.* **24**(2), 117–124 (2016).
85. R. R. Anderson, "Laser medicine in dermatology," *J. Dermatol.* **23**(11), 778–782 (1996).
86. J. A. Parrish and B. C. Wilson, "Current and future trends in laser medicine," *Photochem. Photobiol.* **53**(6), 731–738 (1991).
87. M. L. Wolbarsht and D. H. Sliney, "Laser medicine," *Curr. Opin. Ophthalmol.* **1**(1), 60–63 (1990).
88. A. Vogel and V. Venugopalan, "Mechanisms of pulsed laser ablation of biological tissues," *Chem. Rev.* **103**(2), 577–644 (2003).
89. S. Mallidi et al., "Optical imaging, photodynamic therapy and optically triggered combination treatments," *Cancer J.* **21**(3), 194–205 (2015).
90. E. A. G. Spratt et al., "Phototherapy, photodynamic therapy and photophoresis in the treatment of connective-tissue diseases: a review," *Br. J. Dermatol.* **173**(1), 19–30 (2015).
91. P. Agostinis et al., "Photodynamic therapy of cancer: an update," *CA Cancer J. Clin.* **61**(4), 250–281 (2011).
92. J. Trachtenberg et al., "Vascular targeted photodynamic therapy with palladium-bacteriopheophorbide photosensitizer for recurrent prostate cancer following definitive radiation therapy: assessment of safety and treatment response," *J. Urol.* **178**(5), 1974–1979 discussion 1979 (2007).
93. B. Chen et al., "Combining vascular and cellular targeting regimens enhances the efficacy of photodynamic therapy," *Int. J. Radiat. Oncol. Biol. Phys.* **61**(4), 1216–1226 (2005).
94. F. H. van Duijnhoven et al., "The immunological consequences of photodynamic treatment of cancer, a literature review," *Immunobiology* **207**(2), 105–113 (2003).
95. C. Shi, J. B. Wu, and D. Pan, "Review on near-infrared heptamethine cyanine dyes as theranostic agents for tumor imaging, targeting, and photodynamic therapy," *J. Biomed. Opt.* **21**(5), 050901 (2016).
96. U. Lindner et al., "Image guided photothermal focal therapy for localized prostate cancer: phase I trial," *J. Urol.* **182**(4), 1371–1377 (2009).
97. B. Chen et al., "Vascular and cellular targeting for photodynamic therapy," *Crit. Rev. Eukaryot. Gen. Exp.* **16**(4), 279–306 (2006).

98. M. D. Savellano et al., "Multiepitope HER2 targeting enhances photoimmunotherapy of HER2-overexpressing cancer cells with pyropheorbide-a immunoconjugates," *Cancer Res.* **65**(14), 6371–6379 (2005).
99. M. Del Governatore et al., "Experimental photoimmunotherapy of hepatic metastases of colorectal cancer with a 17.1A chlorin(e6) immunoconjugate," *Cancer Res.* **60**(15), 4200–4205 (2000).
100. T. Harada et al., "Near-infrared photoimmunotherapy with galactosyl serum albumin in a model of diffuse peritoneal disseminated ovarian cancer," *Oncotarget* **7**(48), 79408–79416 (2016).
101. T. Nagaya et al., "Near infrared photoimmunotherapy with avelumab, an anti-programmed death-ligand 1 (PD-L1) antibody," *Oncotarget* **8**(5), 8807–8817 (2017).
102. J. Woodhams et al., "Intracellular re-localisation by photochemical internalisation enhances the cytotoxic effect of gelonin—quantitative studies in normal rat liver," *J. Control Release* **142**(3), 347–353 (2010).
103. D. Ling et al., "Photodynamic efficacy of photosensitizers under an attenuated light dose via lipid nano-carrier-mediated nuclear targeting," *Biomaterials* **33**(21), 5478–5486 (2012).
104. W. Fan et al., "Intranuclear biophotonics by smart design of nuclear-targeting photo-/radio-sensitizers co-loaded upconversion nanoparticles," *Biomaterials* **69**, 89–98 (2015).
105. A. S. Pradhan, J. I. Lee, and J. L. Kim, "Recent developments of optically stimulated luminescence materials and techniques for radiation dosimetry and clinical applications," *J. Med. Phys.* **33**(3), 85–99 (2008).
106. E. G. Yukihara and S. W. McKeever, "Optically stimulated luminescence (OSL) dosimetry in medicine," *Phys. Med. Biol.* **53**(20), R351–R379 (2008).
107. E. C. Pratt, T. M. Shaffer, and J. Grimm, "Nanoparticles and radio-tracers: advances toward radionanomedicine," *Wiley Interdiscip. Rev. Nanomed. Nanobiotechnol.* **8**, 872–890 (2016).
108. H. J. Lee et al., "Synthesis and photoluminescence properties of Eu³⁺-doped silica@coordination polymer core-shell structures and their calcinated silica@Gd₂O₃:Eu and hollow Gd₂O₃:Eu microsphere products," *Small* **9**(4), 561–569 (2013).
109. Y. Zhang et al., "Highly uniform and monodisperse GdOF:Ln³⁺ (Ln = Eu, Tb, Tm, Dy, Ho, Sm) microspheres: hydrothermal synthesis and tunable-luminescence properties," *Dalton Trans.* **42**(39), 14140–14148 (2013).
110. P. Cerenkov, "Visible emission of clean liquids by action of γ radiation," *Doklady Akad. Nauk. SSSR* **2**, 451–454 (1934).
111. P. Cerenkov, "Visible radiation produced by electrons moving in a medium with velocities exceeding the of light," *Phys. Rev.* **52**(4), 378–379 (1937).
112. J. V. Jelley, *Cerenkov Radiation, and Its Applications*, p. 304, Pergamon Press, New York (1958).
113. K. A. Wickersheim, R. V. Alves, and R. A. Buchanan, "Rare earth oxysulfide x-ray phosphors," *IEEE Trans. Nucl. Sci.* **17**(1), 57–60 (1970).
114. H. Yamada et al., "A scintillator Gd₂O₃:Pr, Ce, F for x-ray computed-tomography," *J. Electrochem. Soc.* **136**(9), 2713–2716 (1989).
115. E.-J. Popovici et al., "Synthesis and characterisation of rare earth oxysulphide phosphors. I. Studies on the preparation of Gd₂O₃:Tb phosphor by the flux method," *Opt. Mater.* **27**(3), 559–565 (2004).
116. R. Morlotti et al., "Intrinsic conversion efficiency of X-rays to light in Gd₂O₃:Tb³⁺ powder phosphors," *J. Lumin.* **72**(4), 772–774 (1997).
117. S.-S. Yi et al., "Enhanced luminescence of Gd₂O₃:Eu³⁺ thin-film phosphors by Li doping," *Appl. Phys. Lett.* **84**(3), 353–355 (2004).
118. L. Jacobsohn et al., "Synthesis, luminescence and scintillation of rare earth doped lanthanum fluoride nanoparticles," *Opt. Mater.* **33**(2), 136–140 (2010).
119. C. Dujardin et al., "Luminescence and scintillation properties at the nanoscale," *IEEE Trans. Nucl. Sci.* **57**(3), 1348–1354 (2010).
120. V. N. Makhov et al., "Crossluminescence of nanosized KYF₄," *IEEE Trans. Nucl. Sci.* **59**(5), 2102–2105 (2012).
121. X. Li et al., "Preparation and luminescence properties of Lu₂O₃:Eu³⁺ nanofibers by sol-gel/electrospinning process," *J. Colloid Interface Sci.* **349**(1), 166–172 (2010).
122. M. Kobayashi et al., "Development of vertically aligned ZnO-nanowires scintillators for high spatial resolution x-ray imaging," *Appl. Phys. Lett.* **106**(8), 081909 (2015).
123. J. Wallentin et al., "Hard X-ray detection using a single 100 nm diameter nanowire," *Nano Lett.* **14**(12), 7071–7076 (2014).
124. G. Martínez-Criado et al., "Exploring single semiconductor nanowires with a multimodal hard x-ray nanoprobe," *Adv. Mater.* **26**(46), 7873–7879 (2014).
125. K. D. Steidley, R. M. Eastman, and R. J. Stabile, "Observations of visual sensations produced by Cerenkov radiation from high-energy electrons," *Int. J. Radiat. Oncol. Biol. Phys.* **17**(3), 685–690 (1989).
126. C. E. de Almeida and P. R. Almond, "Energy calibration of high energy electrons using a Cerenkov detector and a comparison with different methods," *Phys. Med. Biol.* **19**(4), 476–483 (1974).
127. J. Axelsson et al., "Cerenkov emission induced by external beam radiation stimulates molecular fluorescence," *Med. Phys.* **38**(7), 4127–4132 (2011).
128. P. J. McNulty, V. P. Pease, and V. P. Bond, "Visual sensations induced by Cerenkov radiation," *Science* **189**(4201), 453–454 (1975).
129. W. C. Haxton, "Salty water Cerenkov detectors for solar neutrinos," *Phys. Rev. Lett.* **77**(8), 1662–1662 (1996).
130. E. Andres et al., "Observation of high-energy neutrinos using Cerenkov detectors embedded deep in Antarctic ice," *Nature* **410**(6827), 441–443 (2001).
131. J. F. Beacom and M. R. Vagins, "Antineutrino spectroscopy with large water Cerenkov detectors," *Phys. Rev. Lett.* **93**(17), 171101 (2004).
132. R. S. Dothager et al., "Cerenkov radiation energy transfer (CRET) imaging: a novel method for optical imaging of PET isotopes in biological systems," *PLoS One* **5**(10), e13300 (2010).
133. L. A. Jarvis et al., "Cherenkov video imaging allows for the first visualization of radiation therapy in real time," *Int. J. Radiat. Oncol. Biol. Phys.* **89**(3), 615–622 (2014).
134. R. Zhang et al., "Cherenkovscopy based patient positioning validation and movement tracking during post-lumpectomy whole breast radiation therapy," *Phys. Med. Biol.* **60**(1), L1–L14 (2015).
135. S. Clement et al., "X-ray induced singlet oxygen generation by nanoparticle-photosensitizer conjugates for photodynamic therapy: determination of singlet oxygen quantum yield," *Sci. Rep.* **6**, 19954 (2016).
136. H. Chen et al., "Nanoscintillator-mediated x-ray inducible photodynamic therapy for in vivo cancer treatment," *Nano Lett.* **15**(4), 2249–2256 (2015).
137. N. Kotagiri et al., "Breaking the depth dependency of phototherapy with Cerenkov radiation and low-radiance-responsive nanophotosensitizers," *Nat. Nanotechnol.* **10**(4), 370–379 (2015).
138. Z. Ouyang et al., "Nanoparticle-aided external beam radiotherapy leveraging the Cerenkov effect," *Phys. Med.* **32**(7), 944–947 (2016).
139. N. Y. Morgan et al., "Nanoscintillator conjugates as photodynamic therapy-based radiosensitizers: calculation of required physical parameters," *Radiat. Res.* **171**(2), 236–244 (2009).
140. A. L. Bulin et al., "Modelling energy deposition in nanoscintillators to predict the efficiency of the x-ray-induced photodynamic effect," *Nanoscale* **7**(13), 5744–5751 (2015).
141. R. Generalov et al., "Radiosensitizing effect of zinc oxide and silica nanocomposites on cancer cells," *Colloids Surf. B* **129**, 79–86 (2015).
142. Y. Tang et al., "Highly efficient FRET system capable of deep photodynamic therapy established on x-ray excited mesoporous LaF₃:Tb scintillating nanoparticles," *ACS Appl. Mater. Interfaces* **7**(22), 12261–12269 (2015).
143. A. Kamkaew et al., "Scintillating nanoparticles as energy mediators for enhanced photodynamic therapy," *ACS Nano* **10**(4), 3918–3935 (2016).
144. S. Kaščáková et al., "X-ray-induced radiophotodynamic therapy (RPDT) using lanthanide micelles: beyond depth limitations," *Nano Res.* **8**(7), 2373–2379 (2015).
145. A.-L. Bulin et al., "X-ray-induced singlet oxygen activation with nanoscintillator-coupled porphyrins," *J. Phys. Chem. C* **117**(41), 21583–21589 (2013).
146. C. Zhang et al., "Marriage of scintillator and semiconductor for synchronous radiotherapy and deep photodynamic therapy with diminished oxygen dependence," *Angew. Chem. Int. Ed.* **54**(6), 1770–1774 (2015).
147. D. R. Cooper, D. Bekah, and J. L. Nadeau, "Gold nanoparticles and their alternatives for radiation therapy enhancement," *Front. Chem.* **2**, 86 (2014).

148. E. Brun, L. Sanche, and C. Sicard-Roselli, "Parameters governing gold nanoparticle x-ray radiosensitization of DNA in solution," *Colloids Surf. B* **72**(1), 128–134 (2009).
149. L. Cui et al., "Hypoxia and cellular localization influence the radiosensitizing effect of gold nanoparticles (AuNPs) in breast cancer cells," *Radiat. Res.* **182**(5), 475–488 (2014).
150. S. Her et al., "Dual action enhancement of gold nanoparticle radiosensitization by pentamidine in triple negative breast cancer," *Radiat. Res.* **185**(5), 549–562 (2016).
151. H. N. McQuaid et al., "Imaging and radiation effects of gold nanoparticles in tumour cells," *Sci. Rep.* **6**, 19442 (2016).
152. X. Ai, J. Mu, and B. Xing, "Recent advances of light-mediated theranostics," *Theranostics* **6**(13), 2439–2457 (2016).
153. F. Almutawa et al., "Efficacy of localized phototherapy and photodynamic therapy for psoriasis: a systematic review and meta-analysis," *Photodermatol. Photoimmunol. Photomed.* **31**(1), 5–14 (2015).
154. A. Mikolajczyk et al., "Evaluating the toxicity of TiO₂-based nanoparticles to Chinese hamster ovary cells and Escherichia coli: a complementary experimental and computational approach," *Beilstein J. Nanotechnol.* **8**, 2171–2180 (2017).
155. D. S. Sun et al., "Visible light-responsive platinum-containing titania nanoparticle-mediated photocatalysis induces nucleotide insertion, deletion and substitution mutations," *Nanomaterials* **7**(1), 2 (2017).
156. R. R. Allison and C. H. Sibata, "Oncologic photodynamic therapy photosensitizers: a clinical review," *Photodiagn. Photodyn. Ther.* **7**(2), 61–75 (2010).
157. L. Colombeau et al., "Inorganic nanoparticles for photodynamic therapy," *Top Curr. Chem.* **370**, 113–134 (2016).
158. L. Larue et al., "Using x-rays in photodynamic therapy: an overview," *Photochem. Photobiol. Sci.* (2018).
159. P. Retif et al., "Nanoparticles for radiation therapy enhancement: the key parameters," *Theranostics* **5**(9), 1030–1044 (2015).
160. A. Dsouza et al., "Cherenkov-excited multi-fluorophore sensing in tissue-simulating phantoms and *in vivo* from external beam radiotherapy," *Radiat. Res.* **189**(2), 197–204 (2018).
161. H. Lin et al., "Comparison of Cherenkov excited fluorescence and phosphorescence molecular sensing from tissue with external beam irradiation," *Phys. Med. Biol.* **61**(10), 3955–3968 (2016).
162. Y. Liu et al., "Investigation of water-soluble x-ray luminescence nanoparticles for photodynamic activation," *Appl. Phys. Lett.* **92**(4), 043901 (2008).
163. X. Zou et al., "X-ray-induced nanoparticle-based photodynamic therapy of cancer," *Nanomedicine* **9**(15), 2339–2351 (2014).
164. A. H. Elmenoufy et al., "A novel deep photodynamic therapy modality combined with CT imaging established via x-ray stimulated silica-modified lanthanide scintillating nanoparticles," *Chem. Commun.* **51**(61), 12247–12250 (2015).
165. J. P. Scaffidi et al., "Activity of psoralen-functionalized nanoscintillators against cancer cells upon x-ray excitation," *ACS Nano* **5**(6), 4679–4687 (2011).
166. B. C. Wilson, M. Jermyn, and F. Leblond, "Challenges and opportunities in clinical translation of biomedical optical spectroscopy and imaging," *J. Biomed. Opt.* **23**(3), 030901 (2018).
167. B. C. Wilson, M. Olivo, and G. Singh, "Subcellular localization of Photofrin and aminolevulinic acid and photodynamic cross-resistance in vitro in radiation-induced fibrosarcoma cells sensitive or resistant to photofrin-mediated photodynamic therapy," *Photochem. Photobiol.* **65**(1), 166–176 (1997).
168. D. Kessel and R. D. Poretz, "Sites of photodamage induced by photodynamic therapy with a chlorin e6 triacetoxymethyl ester (CAME)," *Photochem. Photobiol.* **71**(1), 94–96 (2000).
169. S. Hashiguchi et al., "Acridine orange excited by low-dose radiation has a strong cytotoxic effect on mouse osteosarcoma," *Oncology* **62**(1), 85–93 (2002).
170. T. Matsubara et al., "Methylene blue in place of acridine orange as a photosensitizer in photodynamic therapy of osteosarcoma," *In Vivo* **22**(3), 297–303 (2008).
171. K. Kusuzaki et al., "Clinical trial of photodynamic therapy using acridine orange with/without low dose radiation as new limb salvage modality in musculoskeletal sarcomas," *Anticancer Res.* **25**(2B), 1225–1235 (2005).
172. K. Kusuzaki et al., "Clinical outcome of a novel photodynamic therapy technique using acridine orange for synovial sarcomas," *Photochem. Photobiol.* **81**(3), 705–709 (2005).
173. K. Kusuzaki et al., "Review. Acridine orange could be an innovative anticancer agent under photon energy," *In Vivo* **21**(2), 205–214 (2007).
174. K. Kusuzaki et al., "Clinical trial of radiotherapy after intravenous injection of acridine orange for patients with cancer," *Anticancer Res.* **38**(1), 481–489 (2018).
175. L. Ma et al., "X-ray excited ZnS: Cu, Co afterglow nanoparticles for photodynamic activation," *Appl. Phys. Lett.* **105**(1), 013702 (2014).
176. A. Kamkaew et al., "Cerenkov radiation induced photodynamic therapy using chlorin e6-loaded hollow mesoporous silica nanoparticles," *ACS Appl. Mater. Interfaces* **8**(40), 26630–26637 (2016).
177. C. M. Carpenter et al., "Hybrid x-ray/optical luminescence imaging: characterization of experimental conditions," *Med. Phys.* **37**(8), 4011–4018 (2010).
178. Z. Xue et al., "X-ray activated near-infrared persistent luminescent probe for deep-tissue and renewable *in vivo* bioimaging," *ACS Appl. Mater. Interfaces* **9**(27), 22132–22142 (2017).
179. G. Pratz et al., "Tomographic molecular imaging of x-ray-excitable nanoparticles," *Opt. Lett.* **35**(20), 3345–3347 (2010).
180. D. J. Naczynski et al., "X-ray-induced shortwave infrared biomedical imaging using rare-earth nanoprobles," *Nano Lett.* **15**(1), 96–102 (2015).
181. G. Pratz et al., "X-ray luminescence computed tomography via selective excitation: a feasibility study," *IEEE Trans. Med. Imaging* **29**(12), 1992–1999 (2010).
182. W. Cong et al., "X-ray micromodulated luminescence tomography in dual-cone geometry," *J. Biomed. Opt.* **19**(7), 076002 (2014).
183. W. Zhang et al., "X-ray luminescence computed tomography using a focused x-ray beam," *J. Biomed. Opt.* **22**(11), 116004 (2017).
184. X. Liu et al., "Excitation-resolved cone-beam x-ray luminescence tomography," *J. Biomed. Opt.* **20**(7), 070501 (2015).
185. P. Gao et al., "Resolving adjacent nanophosphors of different concentrations by excitation-based cone-beam x-ray luminescence tomography," *Biomed. Opt. Express* **8**(9), 3952–3965 (2017).
186. H. Zhang et al., "Performance evaluation of the simplified spherical harmonics approximation for cone-beam x-ray luminescence computed tomography imaging," *J. Innovative Opt. Health Sci.* **10**(3), 1750005 (2017).
187. M. A. Lewis et al., "On the potential for molecular imaging with Cerenkov luminescence," *Opt. Lett.* **35**(23), 3889–3891 (2010).
188. G. S. Mitchell et al., "In vivo Cerenkov luminescence imaging: a new tool for molecular imaging," *Philos. Trans. A* **369**(1955), 4605–4619 (2011).
189. Y. Xu, H. Liu, and Z. Cheng, "Harnessing the power of radionuclides for optical imaging: Cerenkov luminescence imaging," *J. Nucl. Med.* **52**(12), 2009–2018 (2011).
190. Y. Xu et al., "Proof-of-concept study of monitoring cancer drug therapy with Cerenkov luminescence imaging," *J. Nucl. Med.* **53**(2), 312–317 (2012).
191. J. L. Demers et al., "Cerenkov excited fluorescence tomography using external beam radiation," *Opt. Lett.* **38**(8), 1364–1366 (2013).
192. Z. Hu et al., "Cerenkov luminescence tomography of aminopeptidase N (APN/CD13) expression in mice bearing HT1080 tumors," *Mol. Imaging* **12**(3), 173–181 (2013).
193. D. Satpati et al., "Cerenkov luminescence imaging of $\alpha_v\beta_6$ integrin expressing tumors using ⁹⁰Y-labeled peptides," *J. Labelled Comp. Radiopharm.* **57**(9), 558–565 (2014).
194. S. Yamamoto et al., "High resolution Cerenkov light imaging of induced positron distribution in proton therapy," *Med. Phys.* **41**(11), 111913 (2014).
195. P. Bruza et al., "Light sheet luminescence imaging with Cerenkov excitation in thick scattering media," *Opt. Lett.* **41**(13), 2986–2989 (2016).
196. R. Zhang et al., "Cerenkov-excited luminescence scanned imaging," *Opt. Lett.* **40**(5), 827–830 (2015).
197. S. R. Ahmed et al., "Radiotherapy-induced Cerenkov luminescence imaging in a human body phantoms," *J. Biomed. Opt.* **23**(3), 030504 (2018).

198. R. Zhang et al., "Oxygen tomography by Cerenkov-excited phosphorescence during external beam irradiation," *J. Biomed. Opt.* **18**(5), 050503 (2013).
199. R. W. Holt et al., "Cerenkov excited phosphorescence-based pO₂ estimation during multi-beam radiation therapy: phantom and simulation studies," *Phys. Med. Biol.* **59**(18), 5317–5328 (2014).
200. B. W. Pogue et al., "Maps of in vivo oxygen pressure with submillimetre resolution and nanomolar sensitivity enabled by Cerenkov-excited luminescence scanned imaging," *Nat. Biomed. Eng.* **2**, 254–264 (2018).
201. J. Axelsson et al., "Quantitative Cerenkov emission spectroscopy for tissue oxygenation assessment," *Opt. Express* **20**(5), 5133–5142 (2012).
202. X. Zhang et al., "Noninvasive measurement of tissue blood oxygenation with Cerenkov imaging during therapeutic radiation delivery," *Opt. Lett.* **42**(16), 3101–3104 (2017).
203. N. J. Crane et al., "Raman imaging demonstrates FGF2-induced craniosynostosis in mouse calvaria," *J. Biomed. Opt.* **10**(3), 031119 (2005).
204. J. A. Timlin et al., "Spatial distribution of phosphate species in mature and newly generated mammalian bone by hyperspectral Raman imaging," *J. Biomed. Opt.* **4**(1), 28–34 (1999).
205. M. V. Schulmerich et al., "Noninvasive Raman tomographic imaging of canine bone tissue," *J. Biomed. Opt.* **13**(2), 020506 (2008).
206. J. L. Demers et al., "Next-generation Raman tomography instrument for non-invasive in vivo bone imaging," *Biomed. Opt. Express* **6**(3), 793–806 (2015).
207. B. W. Pogue et al., "Photodynamic therapy with verteporfin in the radiation-induced fibrosarcoma-1 tumor causes enhanced radiation sensitivity," *Cancer Res.* **63**(5), 1025–1033 (2003).

Brian W. Pogue is MacLean professor of engineering at Dartmouth College, Hanover, New Hampshire, and is an adjunct professor of surgery in the Geisel School of Medicine at Dartmouth. He works in optical applications in medicine, specializing in cancer imaging for surgery, photodynamic therapy and radiation therapy. He has published over 330 peer-reviewed papers and is the editor-in-chief of the *Journal of Biomedical Optics*. He recently founded DoseOptics LLC, making the world's first camera to image radiotherapy.

Brian C. Wilson is a senior research scientist at Princess Margaret Cancer Centre and a professor of medical biophysics, Faculty of Medicine, University of Toronto. He has worked in biophotonics since the early 1980s, doing biomedical physics, initially in radiation therapy and medical imaging. He has authored some 400 peer-reviewed papers, mostly in diagnostic and therapeutic applications of optics, and more recently also nanotechnology, in cancer. He has worked with over 30 companies in the past 25 years and has cofounded two spin-off companies in optical bioimaging.